AMERICAN UNIVERSITY OF BEIRUT

EXPERIMENTAL AND ANALYTICAL INVESTIGATION OF ALTERNATE BLOCK SHEAR FAILURE OF BEAMS IN STEEL MOMENT CONNECTIONS

by
MAZEN BILAL HELWE

A thesis
submitted in partial fulfillment of the requirements
for the degree of Master of Engineering
to the Department of Civil and Environmental Engineering
of the Maroun Semaan Faculty of Engineering and Architecture
at the American University of Beirut

Beirut, Lebanon
August 2018

AMERICAN UNIVERSITY OF BEIRUT

EXPERIMENTAL AND ANALYTICAL INVESTIGATION OF ALTERNATE BLOCK SHEAR FAILURE OF BEAMS IN STEEL MOMENT CONNECTIONS

by

MAZEN BILAL HELWE

Approved by:

Dr. Elie G. Hantouche, Assistant Professor — Advisor
Department of Civil and Environmental Engineering

Dr. George Saad, Associate Professor — Member of Committee
Department of Civil and Environmental Engineering

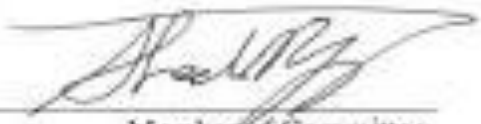

Dr. Shadi Najjar, Associate Professor — Member of Committee
Department of Civil and Environmental Engineering

Date of thesis defense: August 9, 2018

AMERICAN UNIVERSITY OF BEIRUT

THESIS, DISSERTATION, PROJECT RELEASE FORM

Student Name:

El helwe	Mazen	Belal
Last	First	Middle

● Master's Thesis ○ Master's Project ○ Doctoral Dissertation

☐ I authorize the American University of Beirut to: (a) reproduce hard or electronic copies of my thesis, dissertation, or project; (b) include such copies in the archives and digital repositories of the University; and (c) make freely available such copies to third parties for research or educational purposes.

☑ I authorize the American University of Beirut, to: (a) reproduce hard or electronic copies of it; (b) include such copies in the archives and digital repositories of the University; and (c) make freely available such copies to third parties for research or educational purposes
after : **One ---- year from the date of submission of my thesis, dissertation, or project.**

Two ← years from the date of submission of my thesis, dissertation, or project.

Three ---- years from the date of submission of my thesis, dissertation, or project.

M Helwe — Monday, Sept 3rd, 2018

Signature — Date

This form is signed when submitting the thesis, dissertation, or project to the university libraries

ACKNOWLEDGMENTS

First and foremost I would like to thank my thesis advisor Dr. Elie G. Hantouche, for providing all the necessary facilities for the research. The door to Dr. Hantouche office was always open whenever I ran into a trouble or had inquiries about my research work or writing. His expertise, motivation and patience allowed this thesis to be a successful work, he always steered me in the right direction whenever I needed it.

I am also grateful to the experts who were involved in the experimental work for this research work: Mr. Helmi El Khatib, Ms. Dima Al-Hasanieh, and Mr. Abdel Rahman El-Sheikh. I am extremely thankful and indebted to them for sharing expertise, guidance and valuable encouragement extended to me.

My recognition and gratitude are also extended to my committee Dr. George Saad, and Dr. Shadi Najjar.

Furthermore, I would like to gratefully acknowledge the financial support provided by the American University of Beirut Research Board under grant No.21113-102726, and by the Lebanese National Council for Scientific Research (LNCSR) under grant No. 103091-22968.

Finally, I must express my very profound to my family for providing me with unfailing support and encouragement throughout my years of study and through the process of reaching this Master degree. Also I would like to thank my research team and friends for their support, this accomplishment would not have been possible without them. Thank you.

AN ABSTRACT OF THE THESIS OF

Mazen Bilal Helwe for Master of Engineering
Major: Civil and Environmental Engineering

Title: Experimental and Analytical Investigation of Alternate Block shear in steel moment connections

Alternate block shear (ABS) failure in beams needs to be addressed when designing bolted flange plate (BFP) and double Tee moment connections associated with deep beams in seismic areas. This study investigates experimentally and analytically the ABS failure in such moment connections when subjected to monotonic tensile loading. ABS, not yet included in the AISC 358 specifications, is a failure mode that combines full tensile fracture in the beam flange with shear failure in the beam web. The design of BFP and double Tee moment connections requires deep beams and thick plate connections to sustain high moment demands. ABS failure might be considered as one of the potential failure modes in such conditions. Therefore, investigating such failure is necessary for the inclusion in the provisions. To address this issue, FE models are conducted to validate the experimental results of structural Tee connections available in the literature. The same FE technique is conducted on a series of prequalified BFP and double Tee moment connections to examine the ABS failure. The dimensionless ratio of connection length to beam depth ratio is considered the major parameter for identifying the governing failure mode. Then, an experimental program is conducted to examine the ABS failure in the beams associated with thick plate connections. The results of a series of four specimens showed that the ABS failure path is a combination of both yielding and rupture mechanisms leading to a ductile failure in the beam. Moreover, the experimental and FE results conducted in this study are compared with existing strength models to investigate their prediction capability and accuracy while designing moment connections. Results indicate that the ABS failure have a lower capacity than the block shear failure which is included in the ANSI/AISC 358-16 design provisions of the BFP and double Tee connections. FE simulations are developed to predict the experimental results. The FE models can predict with acceptable accuracy the experimental results of force-deformation and the behavior and failure path of the tested specimens. Finally, a proposed methodology is presented through a stiffness based model to predict the failure path and mode in the beam associated with BFP and double Tee moment connections.

The experimental and analytical results clearly show that the ABS failure governs the behavior of beams associated with BFP and double Tee moment connections. These results indicate the importance of including the ABS failure in the design standards to ensure a safe design for steel moment connections. This study will provide design guidelines in predicting the ABS failure mode in steel moment connections. This will constitute a significant change from the current design procedure which doesn't include ABS as a limit state.

CONTENTS

ILLUSTRATIONS

TABLES

ABBREVIATIONS

K_1 : bolt in shear stiffness

d_b : bolt diameter

F_{ub} : ultimate strength of the bolt

d_{M16} : nominal diameter of a M16 bolt

K_2 : plate in bearing stiffness

e_b : edge distance parallel to load transfer

p_b : pitch distance parallel to load transfer

K_3 : web in shear stiffness

β : transformation parameter as defined in the Eurocode 3 (European Committee for standardization CEN, 2005)

z : lever arm (web depth)

E : Young modulus of elasticity

K_4 : web in tension stiffness

d_w : beam web depth

t_w : web thickness

L_c : connection length

K_{ABS} : equivalent stiffness of the connections when ABS is the governing failure mode

K_{NSF} : equivalent stiffness of the connections when NSF is the governing failure mode

K_p : equivalent stiffness of K_1 and K_2 for a single bolt per row

n_b : number of shear bolts per row

$K_{p,ABS}$: post-yielding stiffness of the connections when ABS is the governing failure mode

$K_{p,NSF}$: post-yielding stiffness of the connections when NSF is the governing failure mode

ε : plastic strain of the beam base material

s_{slip} : horizontal distance that bolt can freely slip

d_h : diameter of the bolt hole

A_{gv} : beam gross shear area

A_{nv} : beam net shear area

A_{gt} : beam gross tension area

A_{nt} : beam net tension area

F_y : steel yield stress

F_u : steel ultimate stress

L : total length of the spacing between the bolts

e : beam edge distance

t_w : beam web thickness

A_g : beam gross area

k : fillet distance

R_t : mean stress correction of tension area

R_v : mean stress correction of shear area

CHAPTER I

INTRODUCTION

Steel moment connections are commonly designed by considering a range of potential failure modes, assessing the capacity for each mode, and taking the lowest mode as the governing for the connections. All the other potential failure modes are then compared to the lowest mode and arranged from the lowest to the highest to obtain the sequence of potential failures.

Typical failure modes of beams in steel moment connections include plastic hinging (gross section yielding), net section fracture (NSF), block shear, and bolt tear-out and bearing. However, there are potential failure modes that might occur besides the aforementioned ones. The atypical failure mode in Tees connected through their flange was reported in the literature and termed as ABS. this failure mode is similar to block shear mode which is recognized as a limit state in beams of steel bolted connections as per the ANSI/AISC 358-16 (ANSI/AISC 358, 2016). The failure mechanism of block shear combines a tensile fracture on one plane and shear failure (yielding or rupture) in the transverse plane. The ABS is defined as a combination of full tensile fracture in the beam flange followed by an alternate shear failure path propagating in the beam web toward the edge. Figure 1 shows the block shear and ABS failure in flange plate connected to beam section, representing steel moment connections. The block shear failure is considered a ductile failure mode and is available in the ANSI/AISC 360-16 specifications (ANSI/AISC 360, 2016), unlike the ABS failure which is not recognized as a limit state

In the past two decades, BFP and double Tee moment connections have undergone extensive analytical and experimental investigations to study all potential

failure modes and yielding mechanisms (ANSI/AISC 358, 2016). Such connections undergo significant moment demands requiring deep beams and thick plate connections to sustain the high moment demand. In such conditions, ABS might be a potential failure mode in the beams associated with BFP and double Tee moment connections. In fact, ANSI/AISC 358-16 (ANSI/AISC 358, 2016) explicitly states that ABS failure needs not be checked for the studied connections, since shear bolts are designed to fail prior to net section fracture (NSF) in the beam flange. Recall that NSF in the beam flange occurs during the ABS failure mode (Fig. 1 (b)). However, due to the high moment demand in special moment resisting frames, thick flange plate and Tee stem, and large shear bolts might be needed. This means that NSF in beam flange might occur prior to shear bolt failure. Furthermore, it is evident that block shear failure consists of two shear planes in the beam flange (Fig. 1(a)) while ABS failure consists of one shear plane in the beam web (Fig. 1(b)). Knowing that the beam web thickness is usually less than the beam flange thickness, ABS failure might have a lower capacity than the block shear failure. Therefore, it is essential to investigate experimentally and analytically the ABS failure in beams associated with moment connections. Also, it is important to include ABS failure check in the available design procedure of BFP and double Tee moment connections to ensure a safe design.

Existing experimental and analytical studies dealt only with structural Tee connection to investigate the ABS failure. Figure 1 (c) shows ABS failure path in structural Tee connection. Epstein and McGinnis (1999) developed a series of FE models to reproduce the experimental tests of structural Tee connections (Epstein and McGinnis, 1999). The results showed that the FE simulations were in good agreement with the experimental tests and were capable to predict the governing failure modes. Also, Epstein and Stamberg (2002) conducted an extensive experimental program on structural Tee

connections. Different parameters were incorporated in these tests such as beam depth, eccentricity, connection length, spacing between bolts, and number of bolts. Note that the connection length depends on spacing between bolts and/or number of bolts. It was concluded that as the beam depth increases, the failure mode is controlled by ABS. Similarly, as the connection length decreases, the failure mode is controlled by ABS. Therefore, both beam depth and connection length have been reported in the literature as major behavioral parameters that impact the ABS phenomenon in structural Tee connections. Also, no existing strength model is available in the ANSI/AISC 360-16 specifications (ANSI/AISC 360, 2016) and in the ANSI/AISC 358-16 provisions (ANSI/AISC 358, 2016). The failure mechanism of ABS which is similar to block shear failure has an alternate shear failure path in the beam web as shown in Fig. 1 (a) and (b). Therefore, Epstein 1996 provided a few adjustments on the block shear equations available in the ANSI/AISC 360-16 specifications (ANSI/AISC 360, 2016) and proposed a strength model that predicts the ABS failure capacity for the structural Tee connections (Epstein and McGinnis, 1999 and Epstein and Stamberg, 2002). Moreover, Driver et al. (2005), and Cai and Driver (2010) proposed a *unified* equation (*unified* strength model) that was recommended to be used for all block shear failures, regardless of whether the failure paths are classical (block shear) or atypical (ABS). This equation showed good agreement when compared for many tests of angles, gusset plates, coped beams and tees. The shear term of the *unified* equation was modified with a combination of ultimate and yield stresses.

Despite the experimental and analytical research performed on ABS failure in Tee connections, no research work has been conducted to investigate the ABS failure in beams of full moment connections, specifically BFP and double Tee. Therefore, FE models are developed in this study to investigate the ABS failure on a series of designed

BFP (Sato et al. 2008) and double Tee moment connections (Hantouche, 2010 and Hantouche and Jaffal, 2016). These moment connections were designed following the ANSI/AISC 358-16 specifications (ANSI/AISC 358, 2016) to satisfy the prequalification requirements in special moment resisting frames.

The aim of this research is to investigate experimentally and analytically the ABS failure in beams of BFP and double Tee moment connections when subjected to monotonic tensile loading. First, FE simulations are conducted to validate the experimental results available in the literature (Epstein and McGinnis, 1999). The same FE technique is used to examine the ABS phenomenon in steel moment connections (BFP and double Tee). An extensive parametric study using ABAQUS is conducted by varying the behavioral parameters (connection length and beam depth) that impact the governed failure mode. A dimensionless parameter (connection length to beam depth ratio) is established to classify the governing failure mode (ABS, NSF, or a combination of ABS and NSF). Then, four tests varying the beam depth and the connection length (by varying the number of shear bolts), are performed in the *Structural and Materials Laboratory* at the *American University of Beirut.* FE models are developed again to validate the experimental results. Moreover, the existing strength models that account for the ABS failure are compared with the experimental results available in the literature and the FE results conducted in this study to demonstrate their prediction capabilities. Also, a comparison is made between the ABS and the block shear capacities of the tested specimens to prove that ABS is more critical than block shear and thus needs to be included in the design as a limit state. Finally, to be able to classify the failure path whether it is ABS or NSF, a stiffness based model that characterize the force displacement response of BFP and double Tee moment connection is developed. The proposed stiffness based model is able to predict the governing failure mode based on

the dimensionless ratio (connection length to beam depth ratio) for those moment connection associated with deep beams ranging between W24 and W36. The results of this research will expand the experimental and analytical database of investigating the ABS failure as a limit state in the current design procedure of steel moment connections to ensure a safe design.

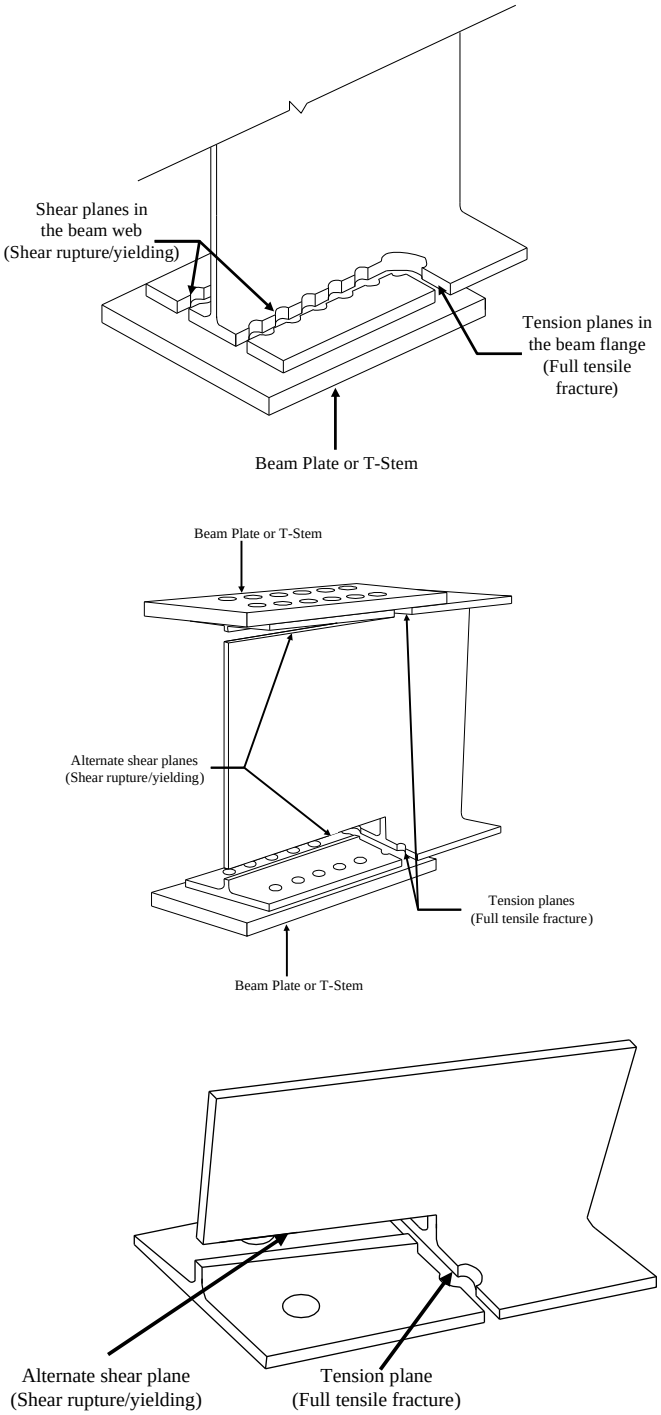

Figure 1. (a) Typical block shear failure in beam associated with steel moment connection, (b) ABS failure path in W beam section associated steel moment connection, and (c) ABS is structural Tee section.

CHAPTER II

FE MODELS OF STRUCTURAL TEE CONNECTIONS AND MOMENT CONNECTIONS (BFP AND DOUBLE TEE)

A. Alternate Block Shear in Structural Tee connections

The FE models are developed to reproduce the structural Tee connections available in Epstein and McGinnis (1999). The results of the structural Tee connections are compared with those obtained from the experimental program and FE results performed by Epstein and McGinnis (1999) as shown in Table 1.

1. Development of FE models

An overall view of the FE model developed in this study using ABAQUS is shown in Fig. 2. Details of the geometrical dimensions and the material properties of the connections can be found in Epstein and McGinnis (1999). Further details of this analysis are available in the following section.

2. Boundary conditions

All the specimens are loaded into two steps. The first step applies a pretension force in the shear bolts. The pretensioning is assigned by subjecting a pressure on the head of the bolts equivalent to the minimum required pretension force specified in the ANSI/AISC 360 specifications (ANSI/AISC 360, 2010). The second step applies a displacement on the tip surface of the beam in *Z direction* as shown in Fig. 2.

Throughout the analysis, boundary conditions are applied on different elements of the structural Tee connection as shown in Fig. 2. During the first step, the shear bolts are restrained against any translaltion to ensure the contact between the bolt nut and the bolt head, and the steel base material. During the second step, only the boundary condition on the beam plate surface is kept active.

3. Material discretization

All the connection components were meshed with eight node brick elements with reduced integration technique (C3D8-R). The mesh configuration of the model is shown in Fig. 2. To improve the accuracy of predictions, a fine mesh was used for the whole connection region. Moreover, a mapped mesh technique was used around the bolt holes to account for stress concentrations and to discretize bolts and their surrounding areas. The contact surfaces are modeled using the surface-to-surface sliding with a coefficient of friction of 0.25. The finite sliding permits sliding separation, and rotation of the contact surfaces.

4. FE predictions vs. existing FE simulations and experimental results

FE models are developed to predict the governing failure modes of the structural Tee connections and are validated against the experimental and FE results available in (Epstein and McGinnis, 1999). The failure is classified as ABS when the shear failure propagates toward the beam web edge after a full tensile fracture of the entire beam flange. Also, NSF is considered when the tensile fracture propagates along the entire beam cross section.

The capability of the ABAQUS model to predict the ABS failure is validated against the experimental and FE results (Epstein and McGinnis, 1999). Figure 3 shows the normalized FE failure load versus the beam depth. The normalized failure load is calculated by dividing the failure load of each specimen by the one resulted from WT4x9 (Epstein and McGinnis, 1999). The FE results conducted in this study show a good agreement with the results presented in (Epstein and McGinnis, 1999). FE models predict well the failure load and the failure mode of the specimens when compared with the experimental results as shown in Table 1. Both FE and experimental results show that as

the beam depth increases, the governed failure mode is ABS. The beam depth is considered one of the major parameters that impact the governed failure mode in structural Tee connections. Moreover, once the governed failure mode is ABS, the increase in the beam depth has no effect on the failure load capacity (see Fig. 3). Moreover, both FE and experimental results show the same transition depth where the failure changes from NSF to ABS (combination of ABS and NSF) as illustrated in Table 1 and Fig. 3. This failure starts as ABS failure and changes to NSF as described in Epstein and McGinnis, (1999). Figure 4 (a) and 4 (b) show the von Mises contour of WT4×9+1 (combination of ABS and NSF failure) and WT4×9+2 (ABS failure), respectively. Thus, the same FE modeling technique can be used to examine the ABS failure in steel moment connection such as BFP and double Tee moment connections.

B. Alternate Block Shear in BFP and double Tee moment connections

1. Development of FE models

Considering the steel moment connections available in the literature (Sato et al. 2008, and Hantouche, 2010 and Hantouche and Jaffal, 2016), six FE models are developed to investigate the ABS failure in BFP and double Tee moment connections having deep beams ranging from W24 to W36 and thick plate connections (see Table 2). The same modeling technique described in the previous section is used to model those steel moment connections (BFP and double Tee). An overall view of a typical FE model of steel moment connection used in this study is shown in Fig. 5.

2. Geometry of connection components

The six specimens (BFP and double tee connections) are associated with deep beams W30×108 (BFP-1), W30×148 (BFP-2), W36×150 (BFP-3), W30×108 (TEE-1), W24×76 (TEE-2), and W36×150 (TEE-3). Details of the connections configuration and

dimensions for both BFP and double Tee connections are found in (Sato et al. 2008, and Hantouche, 2010 and Hantouche and Jaffal, 2016), respectively.

3. FE Results

Figure 6 (a) to 6 (f) show the von Mises stress contours for the beams used in the moment connections. The failure modes results for all the specimens are presented in Table 2. The FE results for all the specimens showed that, the failure modes initiated in the beams. Note that most of the specimens showed a web local buckling before failure occurs. This web local buckling was also observed in the experimental results of the structural Tees (Epstein and Stamberg, 2002).

The FE results show the three different failure modes that might govern the behavior of moment connections (ABS, NSF, and a combination of ABS and NSF). BFP-1 and TEE-3 failed by ABS as shown in Figs. 6 (a) and 6 (b), respectively. It was observed that the failure initiates by a tensile fracture in the beam flange followed by a shear failure path in the beam web. BFP-2 and TEE-2 specimens failed by NSF as shown in Figs. 6 (c) and 6 (d), respectively. It was observed that the beams examined a full tensile fracture along the entire beam section, propagating from the top beam flange toward the bottom beam flange. BFP-3 and TEE-1 specimens failed by a combination of ABS and NSF as shown in Figs. 6 (e) and 6 (f), respectively. It was observed that the failure started in the beams as ABS failure and then changed to NSF.

Table 2 shows the failure mode of BFP and double Tee moment connections using FE models. For instance, for beam depth of 762 mm (30 in.) the FE results show that ABS and NSF governed the behavior of BFP-1 and BFP-2, respectively. This indicates that for both moment connections having the same beam depth, the failure mode changes from ABS to NSF when increasing the connection length. Note that, the connection length is the total spacing between the shear bolts. On the other hand, TEE-

2 have a connection length of 533 mm (21 in.) and a beam depth of 607 mm (23.9 in.) failed in NSF, and TEE-3 have a connection length of 667 mm (26.25 in.) and beam depth of 912 mm (35.9 in.) failed in ABS. This indicates that for the moment connections having large connection length, the failure mode changes from NSF to ABS due to the increase in the beam depth. Consequently, this shows that beam depth and connection length are considered the key parameters in determining the type of failure of beams in moment connection.

Table 1. Experimental results (Epstein and McGinnis, 1999), FE results (Epstein and McGinnis, 1999), and FE results of WT4×9s by varying the beam depth.

Series I Sections[1]	Beam depth mm (in.)	Experimental failure mode[1]	Experimental Failure load[1] KN (kips)	FE failure mode[1]	Normalized FE failure load[4]	FE failure mode	FE failure load KN (kips)	Normalized failure load
WT4×9−1	88 (3)	NSF	592.0 (133.1)	NSF	0.982	NSF	525.9 (118.0)	0.956
WT4×9	103 (4)	NSF	608.5 (136.8)	NSF	1.000	NSF	548.9 (123.4)	1.000
WT4×9+1	127 (5)	NSF[2]	617.0 (138.7)	ABS-NSF	1.023	ABS-NSF	564.0 (126.8)	1.028
WT4×9+2	152 (6)	ABS	612.0 (137.6)	ABS	1.046	ABS	577.8 (129.9)	1.052
WT4×9+3	178 (7)	ABS	NA[3]	ABS	1.063	ABS	581.4 (130.7)	1.059
WT4×9+4	203 (8)	ABS	NA	ABS	1.070	ABS	582.7 (131.0)	1.062
WT4×9+5	229 (9)	ABS	NA	ABS	1.076	ABS	583.1 (131.1)	1.062
WT4×9+6	254 (10)	ABS	NA	ABS	1.079	ABS	583.6 (131.2)	1.063
WT4×9+7	279 (11)	ABS	NA	ABS	1.079	ABS	583.6 (131.2)	1.063
WT4×9+8	305 (12)	ABS	NA	ABS	1.080	ABS	584.5 (131.4)	1.064
WT4×9+11	381 (15)	ABS	NA	ABS	1.083	ABS	585.0 (131.5)	1.065

[1]The tabulated data correspond to the ones available in (Epstein and McGinnis, 1999).
[2] The specimen began to fail along ABS before NSF took place as described in (Epstein and McGinnis, 1999).
[3]Not available.
[4]Failure load of each specimen is divided by the one resulted from WT4×9.

Table 2. Failure modes of BFP and double Tee connections using FE models.

Specimen name	Beam section	Beam depth (d) mm (in.)	Connection length (l) mm (in.)	Plate thickness (t_p) mm (in.)	von Mises Failure mode	Ratio (l/d)
BFP-1	W30×108	757 (29.8)	457 (18)	38 (1-1/2)	ABS in Beam	0.604
BFP-2	W30×148	780 (30.7)	732 (30)	44 (1-3/4)	NSF in Beam	0.977
BFP-3	W36×150	912 (35.9)	686 (27)	44 (1-3/4)	ABS-NSF in Beam	0.752
TEE-1	W30×108	757 (29.8)	610 (24)	32 (1-1/4)	ABS-NSF in Beam	0.805
TEE-2	W24×76	607 (23.9)	533 (21)	22 (7/8)	NSF in Beam	0.879
TEE-3	W36×150	912 (35.9)	667 (26.25)	38 (1-1/2)	ABS in Beam	0.731

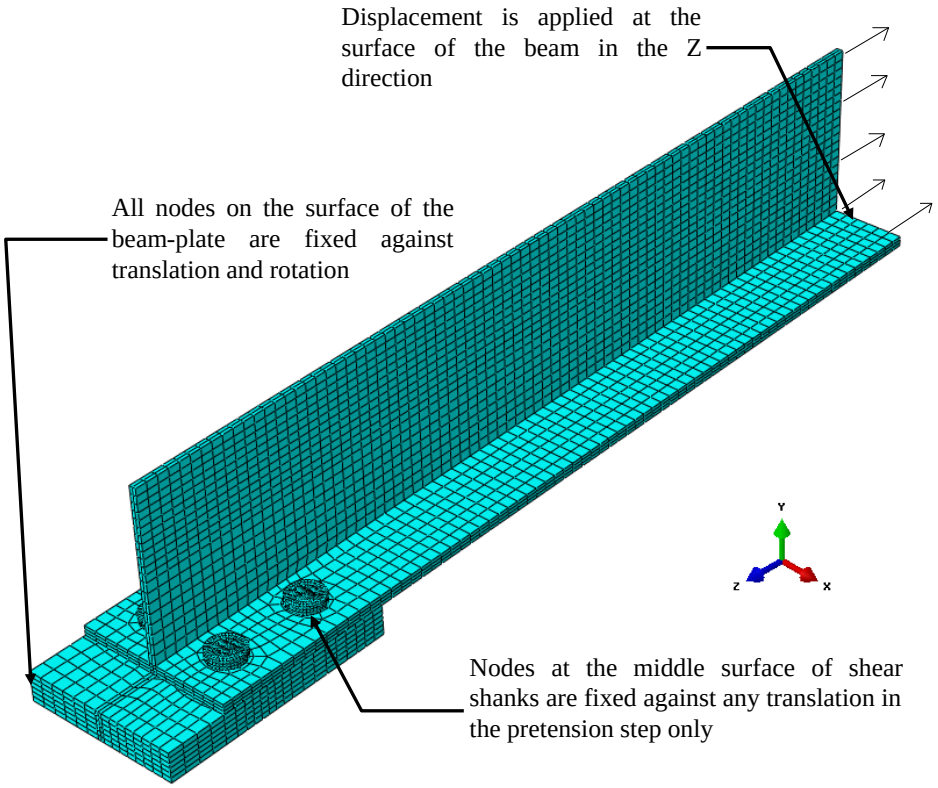

Figure 2. Structural Tee connection details in finite element model.

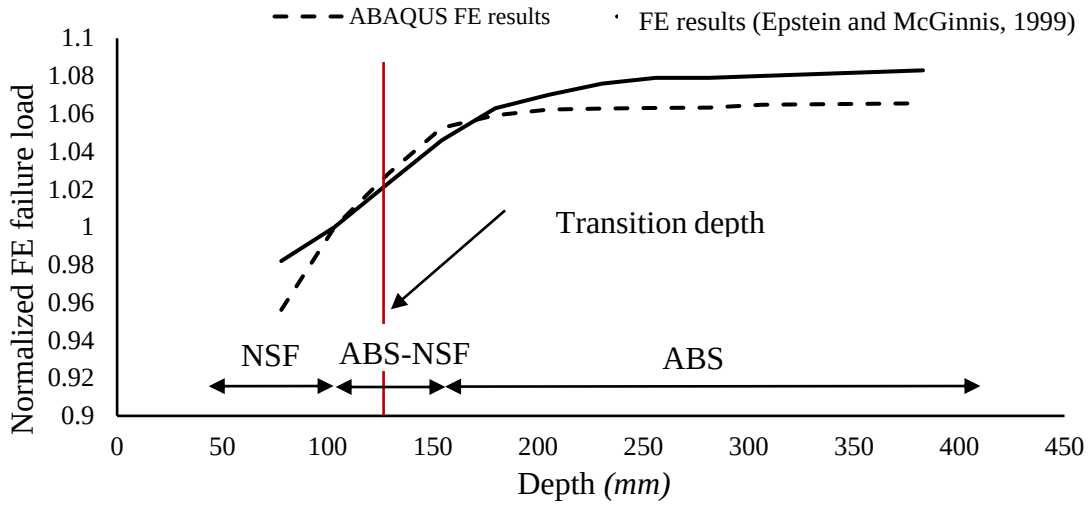

Figure 3. Normalized FE failure loads vs. beam depth: Results of the developed FE vs. existing FE (Epstein and McGinnis, 1999).

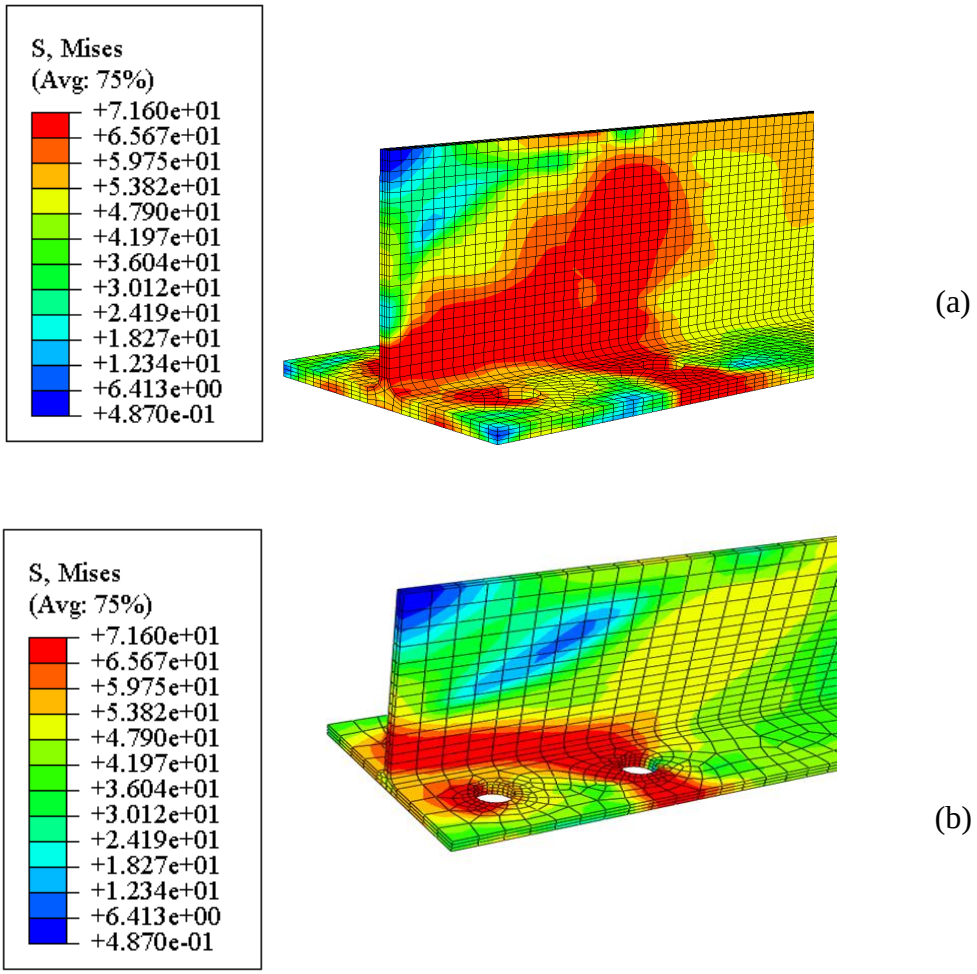

Figure 4. von Mises contour of (a) WT4×9+1, and (b) WT4×9+2.

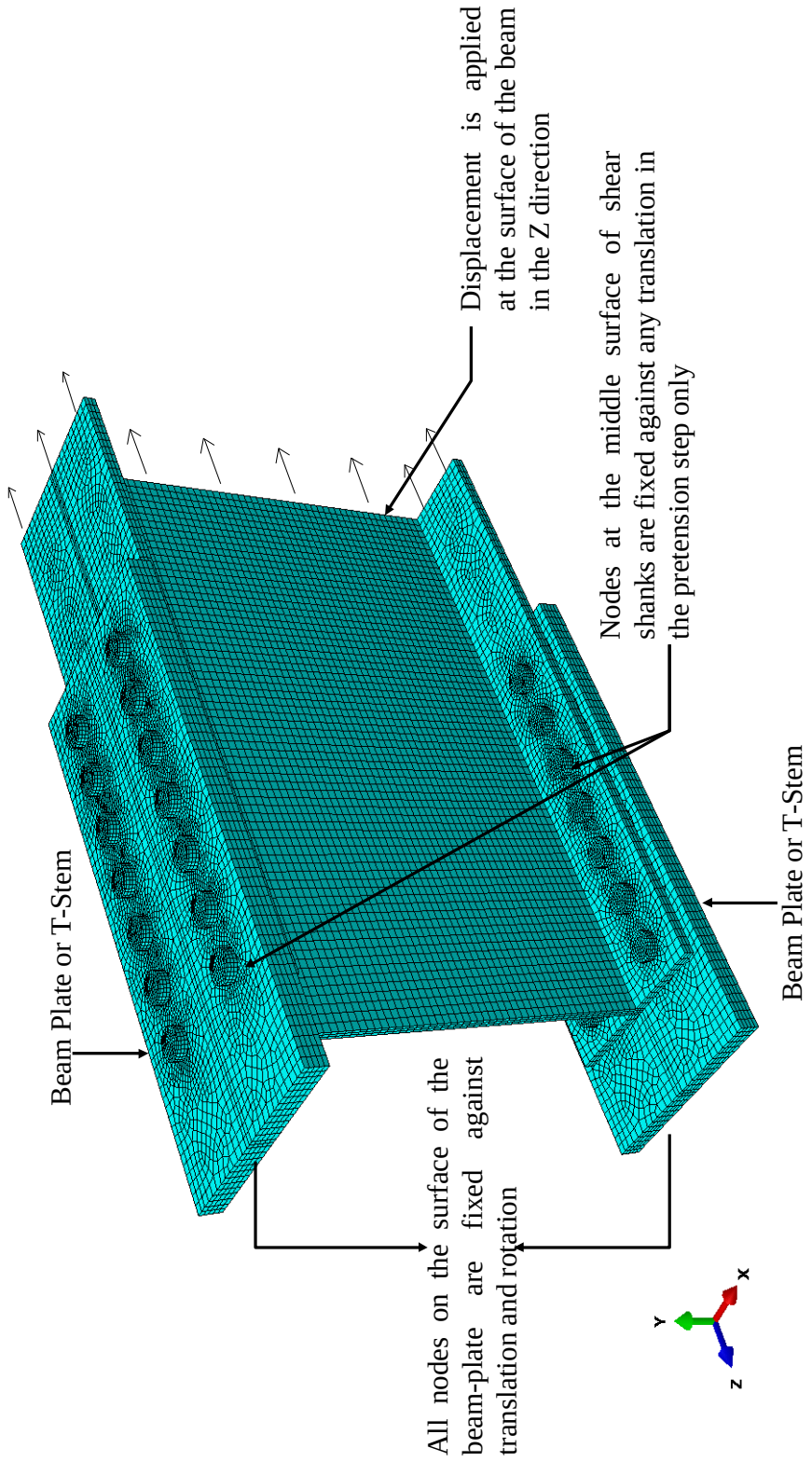

Figure 5. Typical FE model of Steel moment connection (BFP or double Tee).

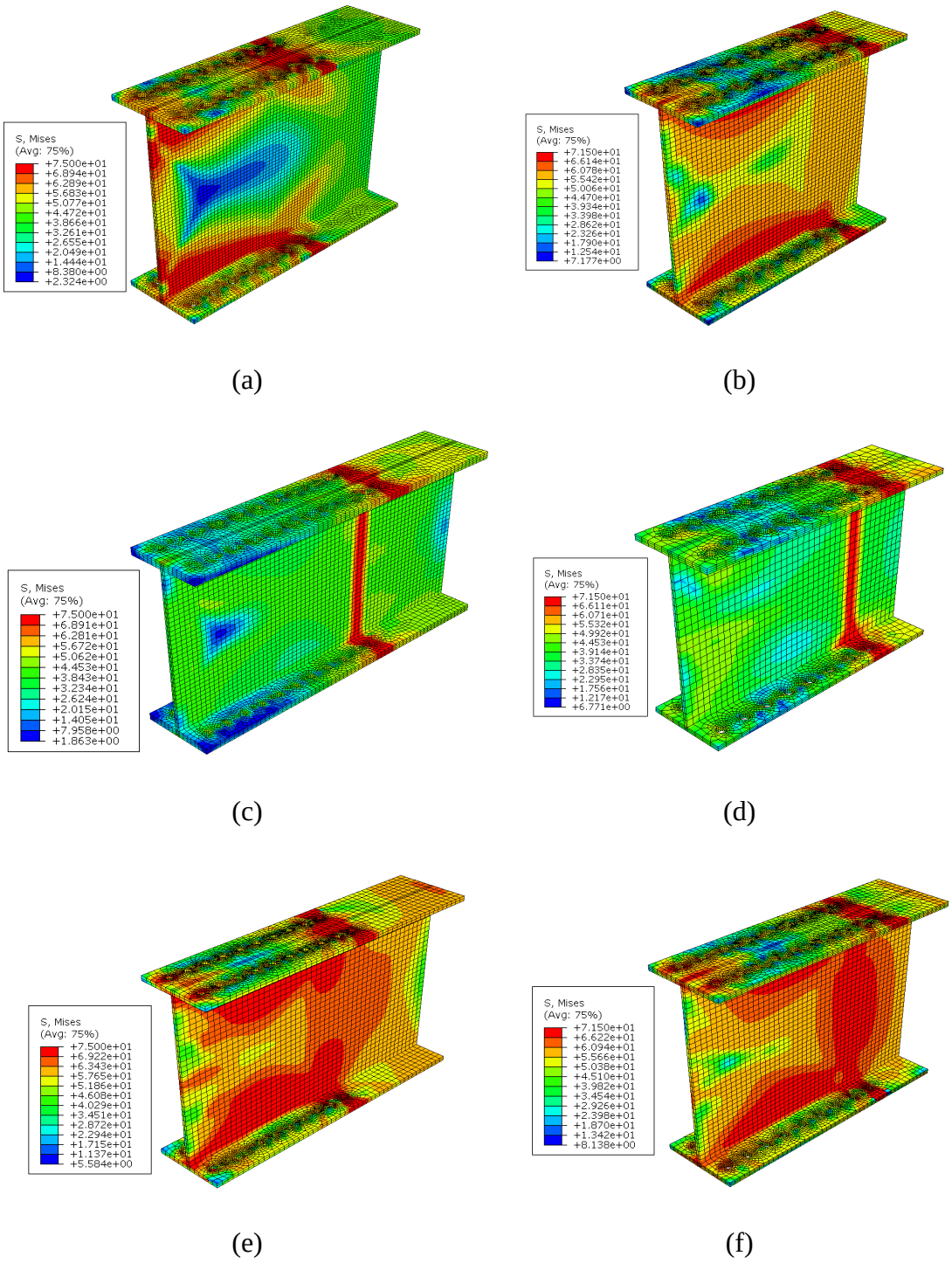

Figure 6. Failure mode of (a) BFP-1, (b) TEE-3, (c) BFP-2, (d) TEE-2, (e) BFP-3, and (f) TEE-1.

CHAPTER III

GEOMETRIC PARAMETERS AFFECTING THE ALTERNATE BLOCK SHEAR IN BPF AND DOUBLE TEE MOMENT CONNECTIONS

The main purpose of this parametric study is to gain additional understanding of the key parameters that impact the behavior of ABS in BFP and double Tee moment connections. Key parameters including the connection length and the beam depth are examined. A dimensionless ratio (connection length to beam depth ratio) is used to classify the beam failure mode. A summary for all the FE results of this parametric study is presented in Table 3, showing the specimens configurations, the failure modes and the connection length to beam depth ratio (l/d).

A. Connection length and beam depth

A study on the effect of connection length and beam depth on BFP and double Tee moment connections behavior is performed. The connection length is varied by whether increasing or decreasing the number of shear bolts in the connections. BFP-1 and TEE-2 are selected for the analyses as shown in Table 3. For BFP-1, the number of shear bolts is increased from 7 to 10 bolts per row. For TEE-2, the number of shear bolts is decreased from 8 to 6 bolts per row. The FE results show that the connection length has a significant effect on the ABS behavior of BFP and double Tee moment connection. It can be concluded that as the connection length decreases, the failure mode is controlled by ABS.

The beam depth is varied by whether increasing or decreasing the beam depth in the connections. BFP-3 and TEE-1 are selected for the analyses as shown in Table 3. For BFP-3, the beam depth is changed from 912 mm (35.9 in.) to 762 mm (30 in.) and 1016 mm (40 in.). For TEE-1, the beam depth is changed from 757 mm (29.8 in.) to 635 mm (25 in.) and 889 mm (35 in.). The results show that the beam depth has a significant effect

on the ABS behavior in BFP and double Tee moment connections. It can be concluded that as the beam depth increases, the failure mode is controlled by ABS.

The results of this study demonstrate that both beam depth and connections length are the major behavioral parameters that impact the ABS failure in BFP and double Tee moment connections. These results conform the conclusions provided by Epstein and McGinnis (1999), and Epstein and Stamberg (2002).

B. Failure criteria

Throughout the studies and the observations, it was clearly recognized that the ABS failure occurred in a sequential manner. The failure initiates by a full tensile fracture in the beam flanges at the location of the leading bolt holes, and then followed by a shear failure propagating in the beam web toward the edge. On the other hand, NSF initiates also by a full tensile fracture in the beam flanges, and then continues along the whole beam web. Therefore, the tensile fracture in the beam flange can be seen as a common initial failure for ABS and NSF.

C. Connection length to beam depth ratio

The connection length to beam depth ratio (l/d) is computed for each case to identify the corresponding governed failure mode as shown in Tables 3. As a result, ABS is the governed failure mode for a ratio (l/d) less than 0.731, whereas NSF is the governed failure mode for a ratio (l/d) larger than 0.879, and a combination of ABS and NSF is the governed failure mode for a ratio (l/d) between 0.731 and 0.879. The connection length to beam depth ratio could be used as a guideline to predict the governed failure mode (ABS, NSF, or combination of ABS and NSF) of BFP and double Tee moment connections associated with deep beams ranging from W24 to W36.

Table 3. Summary of the parametric study results.

Specimen name	Beam section	beam depth (d) mm (in.)	Connection length (l) mm (in.)	Plate thickness (t_p) mm (in.)	von Mises Failure mode	Ratio (l/d)
BFP-1	W30×108	757 (29.8)	457 (18)	38 (1-1/2)	ABS in Beam	0.604
BFP-1-B8	W30×108	757 (29.8)	533 (21)	38 (1-1/2)	ABS in Beam	0.705
BFP-1-B9	W30×108	757 (29.8)	610 (24)	38 (1-1/2)	ABS-NSF in Beam	0.805
BFP-1-B10	W30×108	757 (29.8)	686 (27)	38 (1-1/2)	NSF in Beam	0.906
BFP-3	W36×150	780 (35.9)	686 (27)	44 (1-3/4)	ABS-NSF in Beam	0.752
BFP-3-D30	W36×150	762 (30)	686 (27)	44 (1-3/4)	NSF in Beam	0.900
BFP-3-D40	W36×150	1016 (40)	686 (27)	44 (1-3/4)	ABS in Beam	0.675
TEE-1	W30×108	757 (29.8)	610 (24)	32 (1-1/4)	ABS-NSF in Beam	0.805
TEE-1-D25	W30×108	635 (25)	610 (24)	32 (1-1/4)	NSF in Beam	0.960
TEE-1-D35	W30×108	889 (35)	610 (24)	32 (1-1/4)	ABS in Beam	0.686
TEE-2	W24×76	607 (23.9)	533 (21)	22 (7/8)	NSF in Beam	0.879
TEE-2-B7	W24×76	607 (23.9)	457 (18)	32 (1-1/4)	ABS-NSF in Beam	0.753
TEE-2-B6	W24×76	607 (23.9)	381 (15)	32 (1-1/4)	ABS in Beam	0.628

CHAPTER IV

STIFFNESS BASED MODEL FOR BFP AND DOUBLE TEE MOMENT CONNECTIONS

The purpose of developing the stiffness based model is to determine the failure path and the governing failure mode (ABS or NSF) in BFP and double Tee moment connections. The stiffness based model is able to predict the force displacement characteristics of those moment connections when subjected to tension loading. The proposed stiffness model consists of a series of multi-linear springs that are combined together either in series or in parallel to account for the stiffness of each component in the connections. The assembly of theses springs are illustrated in Fig. 6. The proposed stiffness model is able to predict both the elastic and the plastic stages of the connections. Also, the proposed model is able to account for the force displacement when either ABS or NSF is the governed failure mode. ABS is the governed failure mode when $l / d < 0.731$, and NSF is the governed failure mode when $l / d > 0.879$. BFP-1, BFP-2, and BFP-3-B40 are selected for the analyses. The stiffness components of the connections includes bolts in shear, beam flange and plate in bearing, web in shear, and web in tension as shown in Fig. 6. All the stiffness coefficients of the springs that are incorporated in the stiffness based model are based on the work done by Wuer et al. (2012), and the Eurocode 3 (European Committee for standardization CEN, 2005).

A. Component stiffness

1. Bolts in shear

The bolt in shear stiffness, K_1 is defined as per (Wuer et al. 2012):

$$K_1 = 8d_b^{\,2}\frac{F_{ub}}{d_{M16}} \tag{1}$$

where d_b is the bolt diameter, F_{ub} is the ultimate strength of the bolt, and d_{M16} is the nominal diameter of a M16 bolt. Note that, K_1 is the stiffness of one bolt per row.

2. Plate and beam flange in bearing

The plate in bearing stiffness, and the beam flange in bearing stiffness, K_2 are defined as per (Wuer et al. 2012):

$$K_2 = 12 K_b K_t d_b F_u \tag{2}$$

where K_b is the minimum of K_{b1} and K_{b2}

$$K_{b1} = \frac{0.25 e_b}{d_b} + 0.5 \le 1.25 \tag{3(a)}$$

$$K_{b2} = \frac{0.25 p_b}{d_b} + 0.375 \le 1.25 \tag{3(b)}$$

where e_b is the edge distance parallel to load transfer, and p_b is the pitch distance parallel to load transfer (spacing between bolts).

k_t is taken as the lesser of the two following equations:

$$k_t = \text{lesser of} \begin{cases} \dfrac{1.5t}{d_{M16}} & \text{(4a)} \\ 2.5 & \text{(4b)} \end{cases}$$

where t is the beam flange thickness "t_f" and/or the thickness of the plate/T-stem "t_p" when computing for the bearing stiffness, K_2 of the beam flange and/or the plate/T-stem, respectively.

3. Web in shear

The web in shear stiffness, K_3 is defined as per the Eurocode 3 (European Committee for standardization CEN, 2005):

$$K_3 = \frac{0.38 A_{vw}}{\beta d_w} E \tag{5}$$

where β is the transformation parameter as defined in the Eurocode 3 (European Committee for standardization CEN, 2005), d_w is the beam web depth, A_{vw} is the shear area in the web, and E is the Young modulus of elasticity.

4. Web in tension

The web in tension stiffness, K_4 is defined as per the Eurocode 3 (European Committee for standardization CEN, 2005):

$$K_4 = \frac{0.7 d_w t_w}{l} E \tag{6}$$

where d_w is the beam web depth, t_w is the web thickness, and l is the connection length.

B. Equivalent connection stiffness

The equivalent stiffnesses of BFP, K_{ABS} and K_{NSF}, are defined by assembling the stiffness of each component as presented in Fig. 6. K_{ABS} is the equivalent stiffness of the connections when ABS is the governing failure mode and consists of two parallel springs K_p and K_3. K_{NSF} is the equivalent stiffness of the connection when NSF is the governed failure mode and consists of two parallel springs K_p and K_4. Note that, K_p is developed by assembling the component stiffnesses of the plate- beam flange based on the work done by Wuer et al. (2012) (see Fig. 6). The equivalent stiffness, K_p of a single bolt-row can be expressed:

$$\frac{1}{K_p} = \left(\frac{1}{K_1} + \frac{1}{K_2} + \frac{1}{K_2} \right) \tag{7}$$

The equivalent stiffness, K_{ABS} of BFP can be written as follows:

$$K_{ABS} = 2 n_b K_p + K_3 \tag{8}$$

where n_b is the number of shear bolts per row. It is important to note that, n_b is limited to a maximum number of 7 bolts per row as per (Wuer et al. 2012).

The equivalent stiffness, K_{NSF} of BFP can be expressed as follows:

$$K_{NSF} = 2n_b K_p + K_4 \tag{9}$$

C. Limit states and failure modes

The capacity of each spring component is incorporated in the stiffness model by calculating all limit states and possible failure modes in BFP connections. This includes bolt slip, bolt shear strength, plate bearing resistance, block shear rupture, NSF, and ABS failure. ABS capacity is calculated based on the *unified* equation (Driver et al. 2005 and Cai and Driver, 2010), and the remaining failure modes are calculated based on the equations available in The ANSI/AISC 360 specifications (ANSI/AISC 360, 2016). The failure point on the curve is computed when the moment connection reaches the maximum load capacity that can sustain. In this study, the governing failure modes are either ABS or NSF. When the ABS yielding capacity of the connection is reached, the post-yielding stiffness, $K_{p,ABS}$ is expressed by:

$$K_{p,ABS} = K_{ABS} \frac{F_u - F_y}{\varepsilon E} \tag{10}$$

where ε , is the plastic strain of the beam base material.

When the NSF yielding capacity of the connection is reached, the post-yielding stiffness, $K_{p,NSF}$ is expressed by:

$$K_{p,NSF} = K_{NSF} \frac{F_u - F_y}{\varepsilon E} \tag{11}$$

Moreover, the proposed model is able to predict the slip phase that starts when it reaches the slip resistance force available in the AISC specifications (AISC, 2016) with a displacement, s_{slip} that can be computed as follows:

$$s_{slip} = 2\left(\frac{d_h - d_b}{2}\right) \quad (12)$$

where s_{slip} is the horizontal distance that the bolt can freely slip before having contact with the bolt edge hole and d_h is the diameter of the bolt hole. The failure point in the curve is reached when the force reaches the ABS capacity load or the NSF capacity load.

D. Model performance

The performance of the stiffness based model is validated against the FE results of the BFP connections. Figure 8 shows the force displacement response of the three moment connections (BFP-1, BFP-2, and BFP-3-D40). It can be seen that the proposed model predicts the force displacement with excellent agreement when compared with FE results for all the cases presented. Moreover, the model is able to predict the possible limit states, failure modes (ABS and NSF), and failure displacements.

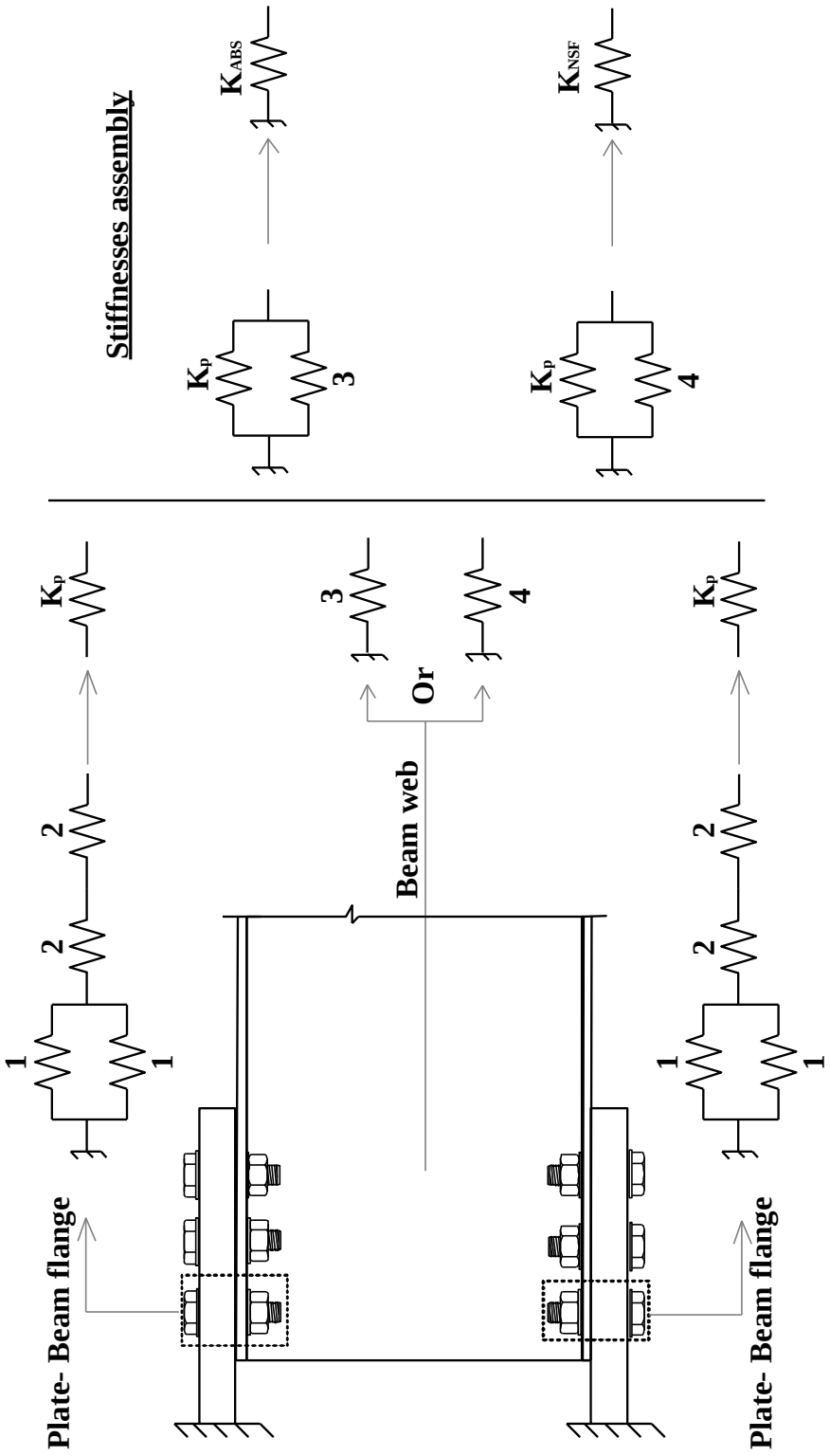

Figure 7. Stiffness model components.

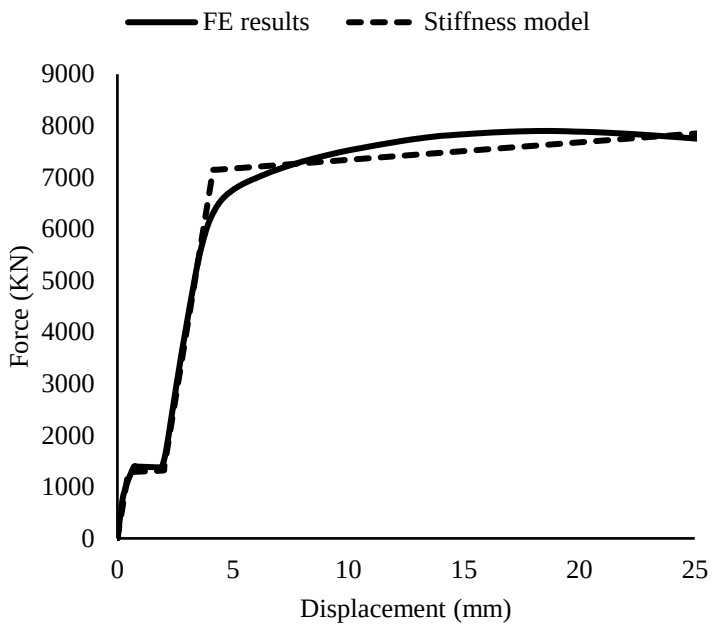
FE results
Stiffness model
9000
8000
7000
6000
5000
4000
3000
2000
1000
0
Force (KN)
0
5
10
15
20
25
Displacement (mm)

(a)

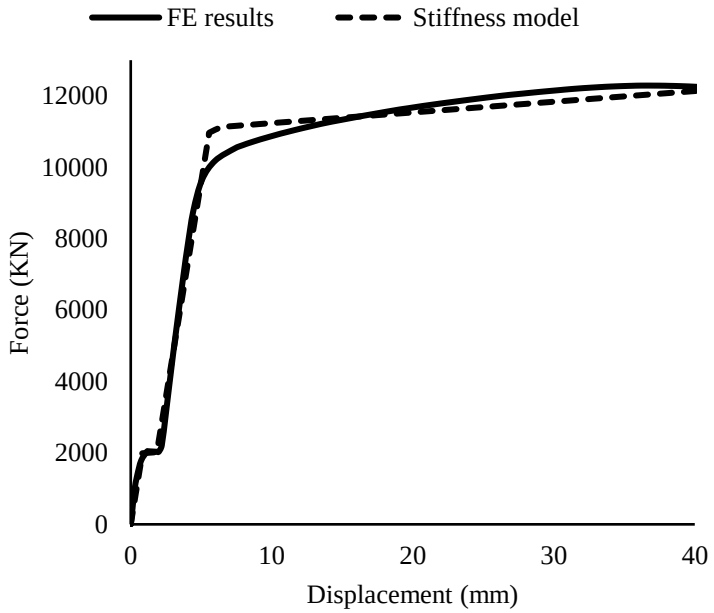
FE results
Stiffness model
12000
10000
8000
6000
4000
2000
0
Force (KN)
0
10
20
30
40
Displacement (mm)

(b)

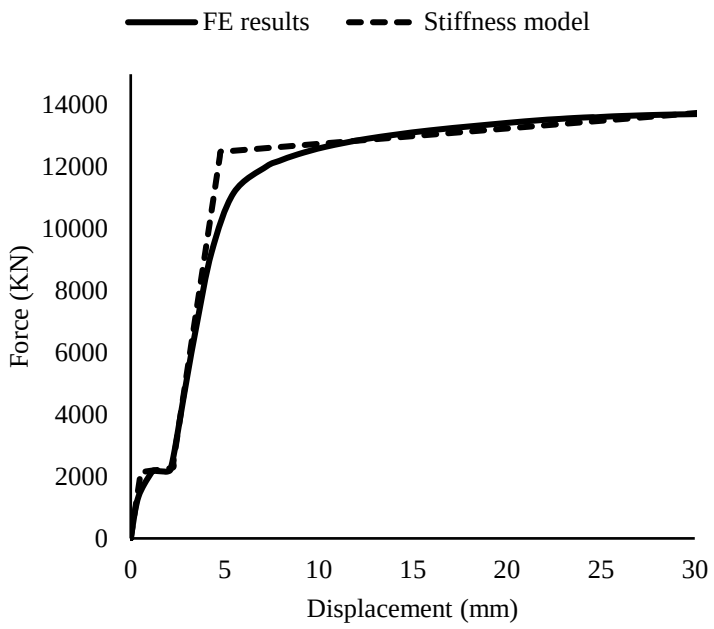

(c)

Figure 8. Stiffness based models vs. FE of BFP moment connections for (a), BFP-1, (b) BFP-2, and (c) BFP-3-D40.

CHAPTER V

EXPERIMENTAL INVESTIGATION OF ALTERNATE BLOCK SHEAR IN STEEL MOMENT CONNECTIONS

A. Experimental program

In order to investigate the strength and behavior of ABS failure mode in beams of BFP and double Tee moment connections, a number of experimental tests were carried out as part of this research. Test specimens were designed to examine the effects of two parameters (connection length and beam depth) on the ABS failure mode and connection strength. The objectives of this experimental program are to: (1) expand the pool of available experimental data , (2) assess the ability of the existing strength models to predict the capacity of ABS in beams of moment connections, (3) provide data to develop and calibrate FE models describing the behavior of ABS in beams associated with moment connections.

To fulfill the above mentioned objectives, four component tests of thick plate connected to beam section were tested under monotonic loading. The beam sections used in the experiment are: IPE 220 (two specimens), IPE 240 (one specimen), and IPE 270 (one specimen). The experimental 2 results conducted in this study can be used as a benchmark for future experimental tests on full scale beams associated with BFP and double Tee moment connections.

B. Test geometry and material properties

One of the objectives of this research is to identify the geometric parameters that affect the ABS failure mode in moment connections. For this purpose, beam depth and number of shear bolts were varied. These parameters were reported in the literature to impact the ABS failure mode. Details of the main geometric and material characteristics of the specimens are presented in Fig. 9 and Table 4. For specimens MC1, MC2, and

MC3 having the same number of shear bolts (3 bolts per row), the beam depth was varied using different beam sections (IPE 220, IPE 240, and IPE 270, respectively). For specimen MC4 having the same beam section as MC1, the number of shear bolts was increased to 4 bolts per row. The flange plate thickness used was 25 mm (1 in.).

The component beams were connected to thick plates (S355) using M18 and M20 (grade 10.9) shear bolts. For all specimens, MC4, taken as a reference specimen, was designed to fail by NSF in the beam and MC1, MC2, and MC3 were designed to fail by ABS in the beam.

C. Experiment setup and test arrangement

An overall view of the test set-up and a schematic drawing of the test assembly configuration are shown in Fig. 10. Six linear variable differential transformers (LVDTs) were used to record the beam deformation throughout the test. LVDTs 1 and 2 were installed to record any deformation at the restrained surface of the specimen, and LVDTs 3, 4, 5, and 6 were installed to record the deformation at the displaced surface of the specimen as shown in Fig. 11. The total displacement in the beam was computed as the deduction of the average of LVDTs 1 and 2 from the average of LVDTs 3 till 6.

D. Loading conditions

Shear bolts in all specimens were preloaded, using direct torque control, in accordance with the minimum pretension load available by the ANSI/AISC 360-16 (ANSI/AISC 360, 2016).

The specimens were subjected to monotonic tensile loading ranging from 1 to 4 mm/min.

C. Test results

Two different failure modes occurred in the experimental program: ABS and NSF. Two limit were reached prior to failure in all specimens: (1) shear bolts slip

occurred at an early stage of the testing and (2) beam web local buckling occurred right after. Note that, beam web local buckling was also observed in the experimental tests of structural Tees (Epstein and Stamberg 2002).

Table 1 summarizes the test results showing the failure mode, the ultimate load that the specimen sustained, and the connection length to beam depth ratio (l/d). This ratio was calculated by dividing the connection length (total spacing between bolts) by the beam depth. Figures 12 and 13show the force-displacement response and the failure path of the specimens, respectively. The results showed that specimens MC1, MC2, and MC3 failed by ABS in the beam section while specimen MC4 failed by NSF. The ultimate displacement recorded at failure point was around 22 mm (0.86 in.) for the beam sections that failed by ABS and 15 mm (0.60 in.) for the beam section that failed by NSF (see Fig. 12). Also, the strain energy (indicated by the area under the force-displacement curve) consumed by the beam sections that failed by ABS is greater than the one consumed by the beam that failed by NSF. This shows that ABS failure is more ductile than NSF.

Figure 13 (a) shows a close-up view of the ABS fracture path in MC3. It is observed that the failure starts by a full tensile fracture in the beam flange, followed by shear failure in the beam web toward the edge. Note that the observed shear failure combines both shear yielding and shear

Table 4. Test results

Section Name	Beam section	Bolts per row	Beam Depth, d, mm (in.)	Connection length, l, mm (in.)	Ratio (l/d)	Failure mode	Failure Load KN (kips)
MC1 (ST44)	IPE220	3	220 (8.66)	100 (3.94)	0.454	ABS	1141 (257)
MC2 (S355)	IPE240	3	240 (9.45)	100 (3.94)	0.416	ABS	1171 (263)
MC3 (ST44)	IPE270	3	270 (10.63)	110 (4.32)	0.407	ABS	1574 (254)
MC4 (ST44)	IPE220	4	220 (8.66)	165 (6.48)	0.750	NSF	1347 (303)

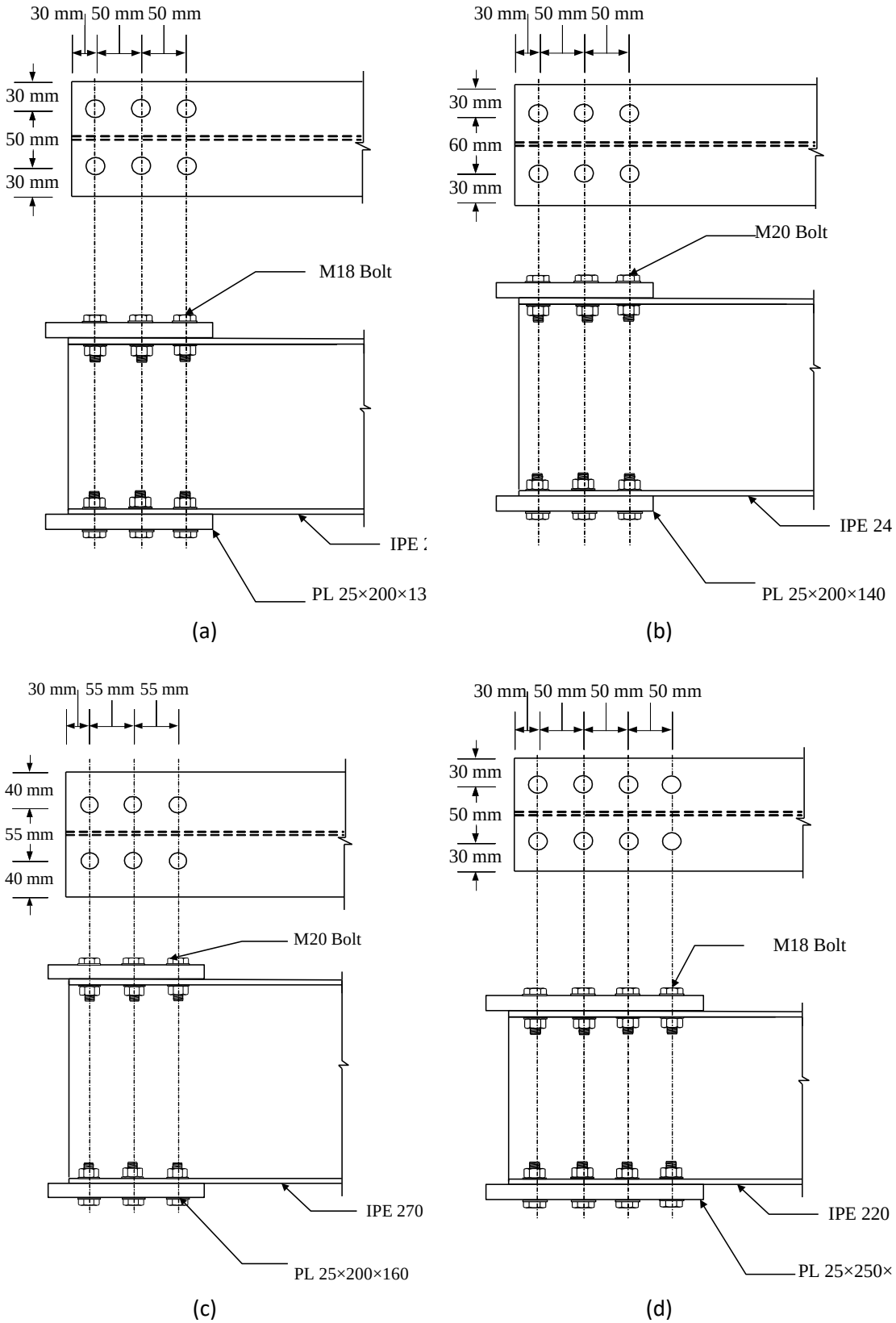

Figure 9. Detailing of (a) MC1, (b) MC2, (c) MC3, and MC4

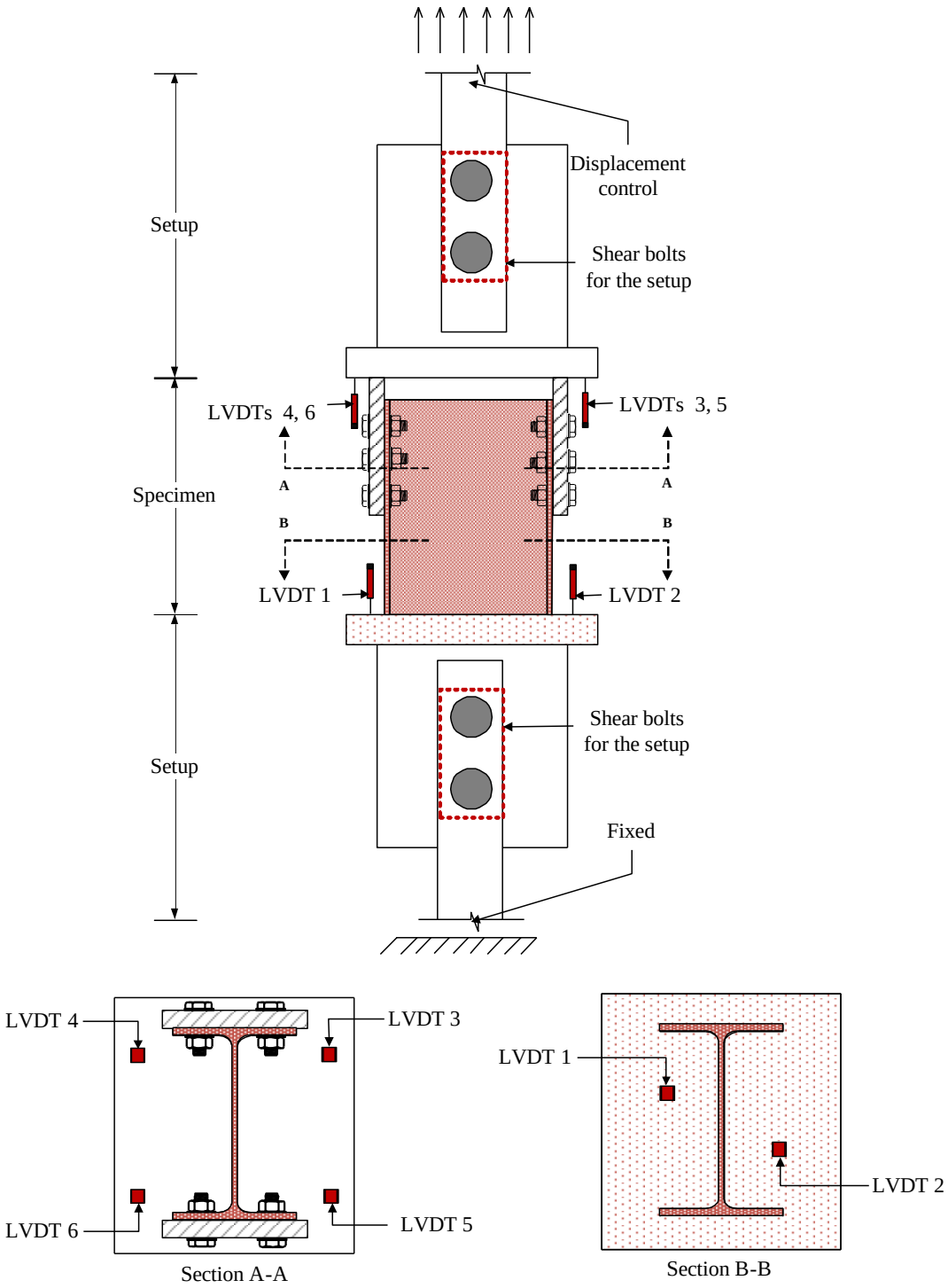

Figure 10. Detailing of the setup and LVDT's distribution.

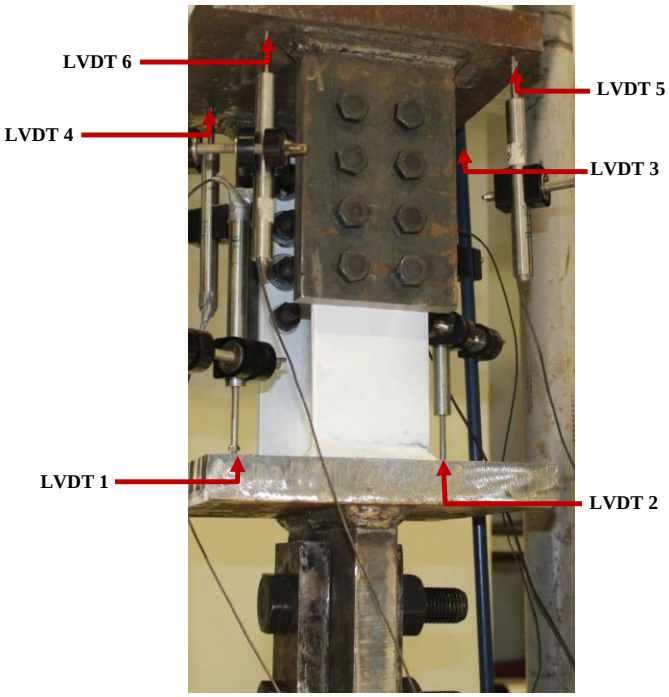

Figure 11. LVDT's configuration.

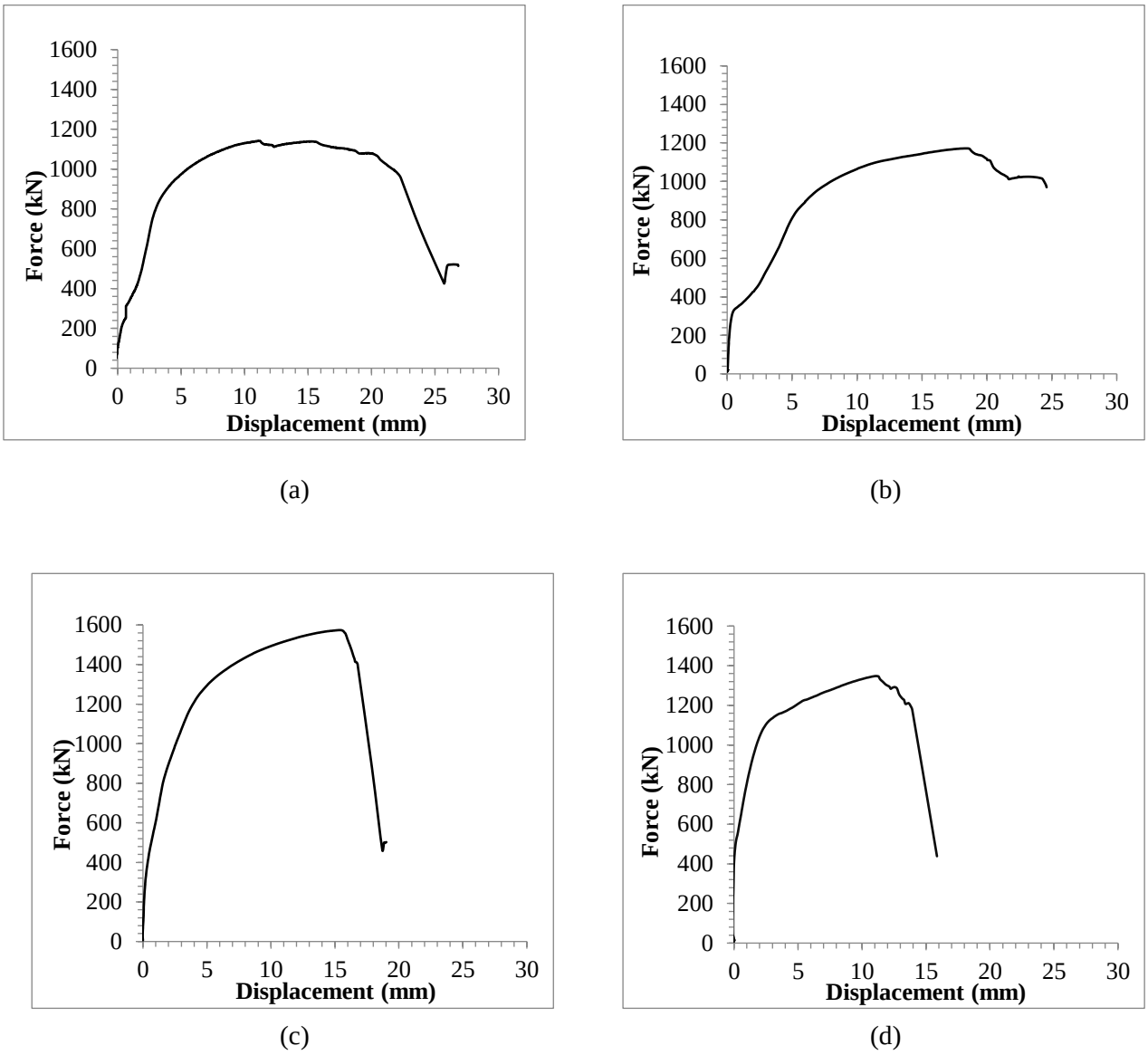

Figure 12. Force displacement response of (a) MC1, (b) MC2, (c) MC3, and (d) MC4.

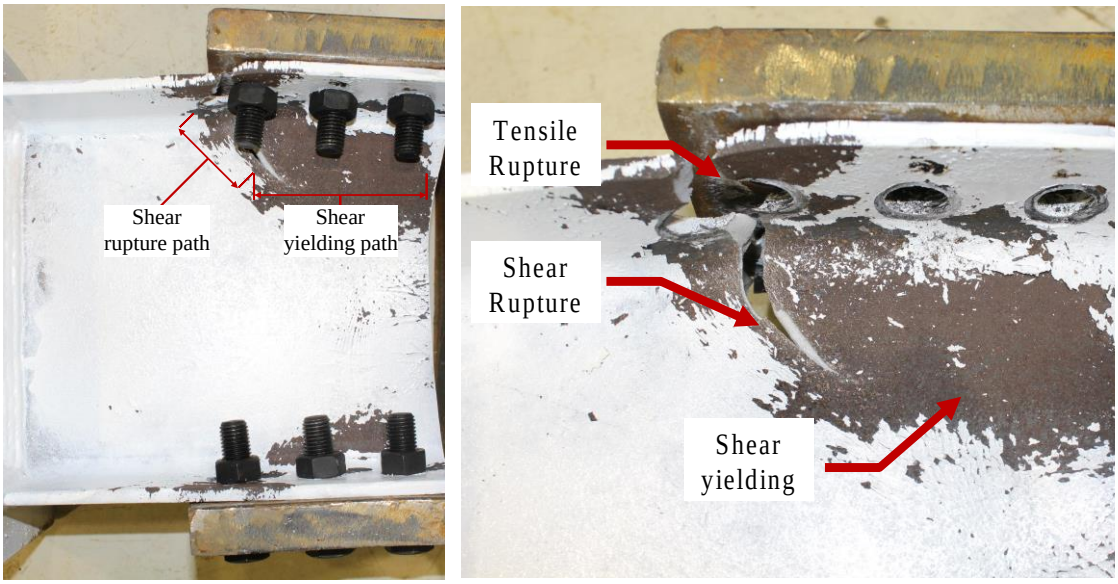

(a)

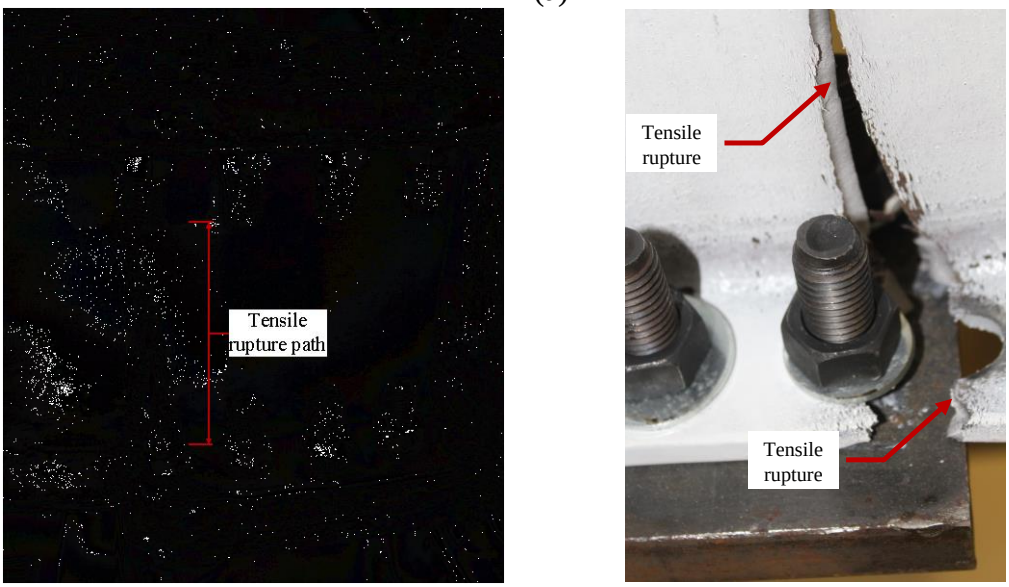

(b)

Figure 13. Experimental failure path: (a) ABS in MC3 specimen, and (b) NSF in MC4 specimen.

CHAPTER VI

FE MODELS VS. EXPERIMENTAL RESULTS

The FE models are developed to reproduce the four tested specimens (MC1, MC2, MC3, and MC4). The results of the FE simulations are compared with the experimental program conducted in the *Structural and Materials Laboratory* at the *American University of Beirut.*

A. Development of FE models

An overall view of the FE model developed in this study using ABAQUS is shown in Fig. 14. The FE models reproduce the geometry details and the material properties of all components, the pre-tensioning of bolts, and the contact interactions at interfaces. The results presented in this chapter are used to better understand the ABS failure mode. Further details of this analysis are available in the following sections.

1. Material properties used for modeling

The von Mises yield criterion is used in this study to model yielding and isotropic hardening to model plastic behavior of the specimens. The bolts used are 10.9 equivalent to A490. The bolt material is used in the FE analysis with a yield stress of 931 Mpa (135 ksi), ultimate stress of 1103 Mpa (160 ksi), and ultimate plastic strain of 0.0103. In this study, the bolts are modelled using their gross area, rather than their effective area. For the base material, ST44 is used for the beams. Note that the true stress and strain for ST44 material is computed and used in the model to get the most accurate results in the

simulations. The true stress strain curve of ST44 is shown in Fig. 15. For all members of the connections, Young's modulus of elasticity is used as E = (29,000 ksi) and Poisson's ratio of $\upsilon = 0.3$. In summary, a bilinear model with isotropic hardening was used for the bolt material, and the true stress strain curve of ST44 for the beam material was used in the analysis.

2. Loading and boundary conditions

All the specimens are loaded into two steps. The first step applies a pretension force in the shear bolts. The pretensioning is assigned by subjecting a pressure on the head of the bolts equivalent to the minimum required pretension force specified in the ANSI/AISC 360 specifications (ANSI/AISC 360, 2010). The second step applies a displacement on the tip surface of the beam in *Z direction* as shown in Fig. 14.

Throughout the analysis, boundary conditions are applied on different elements of the structural Tee connection as shown in Fig. 14. During the first step, the shear bolts are restrained against any translaltion to ensure the contact between the bolt nut and the bolt head, and the steel base material. During the second step, only the boundary condition on the beam plate surface is kept active.

3. Material discretization

All the connection components were meshed with eight node brick elements with reduced integration technique (C3D8-R). The mesh configuration of the model is shown in Fig. 14. To improve the accuracy of predictions, a fine mesh was used for the whole connection region. Moreover, a mapped mesh technique was used around the bolt holes to account for stress concentrations and to discretize bolts and their surrounding areas. The contact surfaces are modeled using the surface-to-surface sliding with a coefficient

of friction of 0.25. The finite sliding permits sliding separation, and rotation of the contact surfaces.

4. Comparison of FE models with experimental results

FE models are developed to validate the failure mode, the failure load, and the force displacement of the experimental results of the tested specimens (MC1, MC2, MC3, and MC4). The failure is classified as ABS when the shear failure propagated in the beam web toward the edge after a full tensile fracture of the beam flange. NSF is considered when a full tensile fracture occurs in the beam cross section.

The values obtained for failure mode, and failure load from FE and experimental tests are compared in Table 5. Result show that FE results are in excellent agreement with the experimental results in predicting the failure mode that governed the behavior of the beams in the moment connections. Also, the FE results can accurately predict the ultimate failure load that the specimen could sustain. It can be seen that the mean value of the tested-to-predicted ratio is very close to 1.0 (see Table 5).

The force displacement curve obtained from the FE analysis for the four specimens is compared with the experimental results, as shown in Fig. 16. The FE results show an excellent agreement with the experimental results (see Fig. 16). The FE models can accurately predict the force displacement behavior, the yielding point, and the fracture point as presented in Fig 16.

The von Mises stress contours for the beams is presented and compared with the experimental results as shown in Fig 17. It can be seen that the FE results can accurately trace the failure path in the beams whether it is ABS or NSF.

Table 5. Summary and FE results (failure mode, failure load, test-to-predicted ratio) of the modeled specimens.

Section Name	**Beam section**	**Bolts per row**	**Beam Depth *d***	**Connection length *l***	**Ratio (l/d)**	**Failure mode**	**Failure Load**		**T/P**
							Experiment ***(KN)***	**FE** ***(KN)***	
MC1	IPE220	3	8.66" (220)	3.94" (100)	0.454	ABS	1141	1164	0.980
MC2	IPE270	3	10.63" (270)	4.32" (110)	0.407	ABS	1574	1608	0.979
MC3	IPE240	3	9.45" (240)	3.94" (100)	0.416	ABS	1171	1216	0.963
MC4	IPE220	4	8.66" (220)	6.48" (165)	0.750	NSF	1347	1358	0.992
Mean T/P									0.979

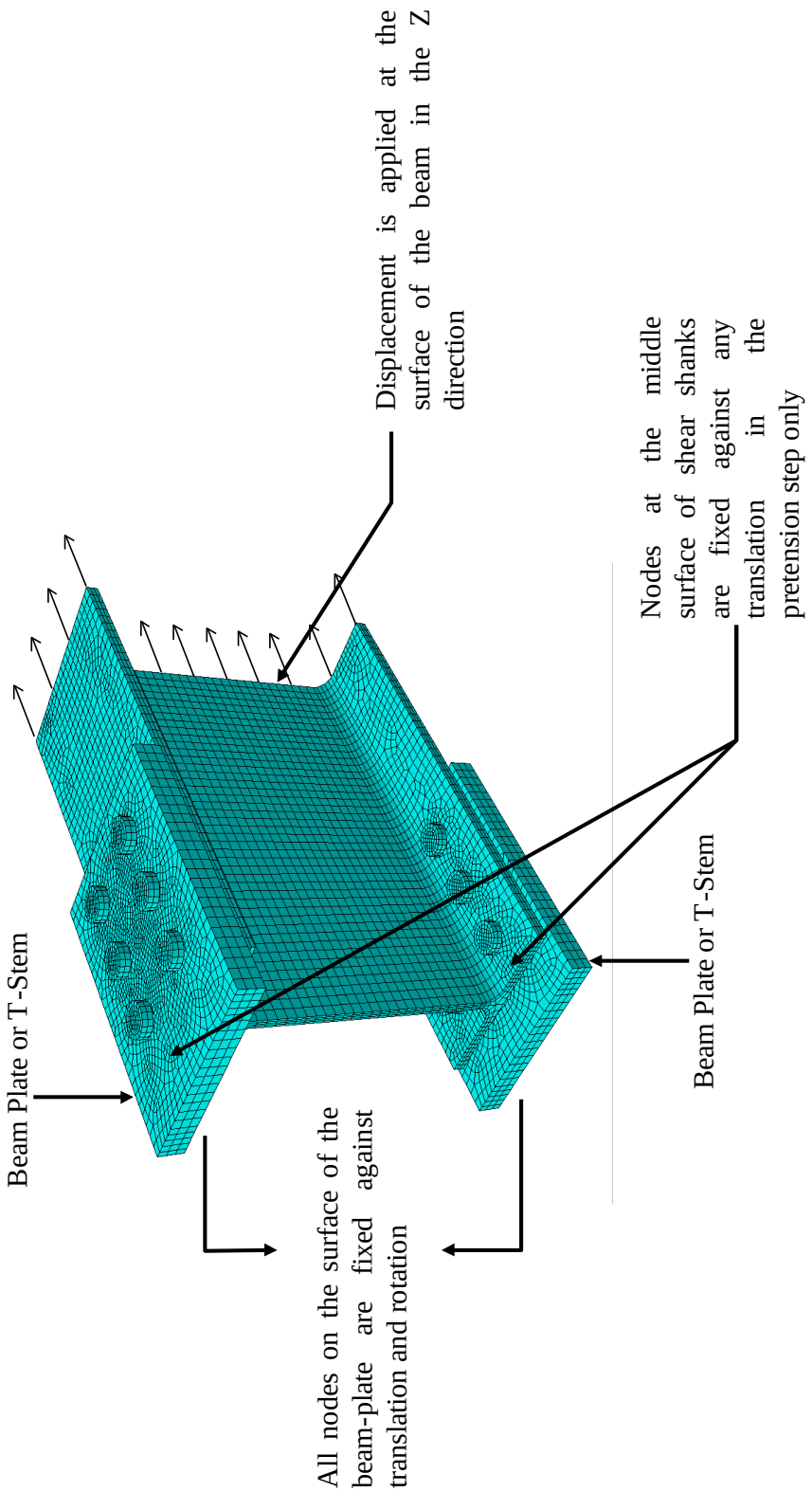

Figure 14. Typical FE model of the specimens (BFP/ double Tee).

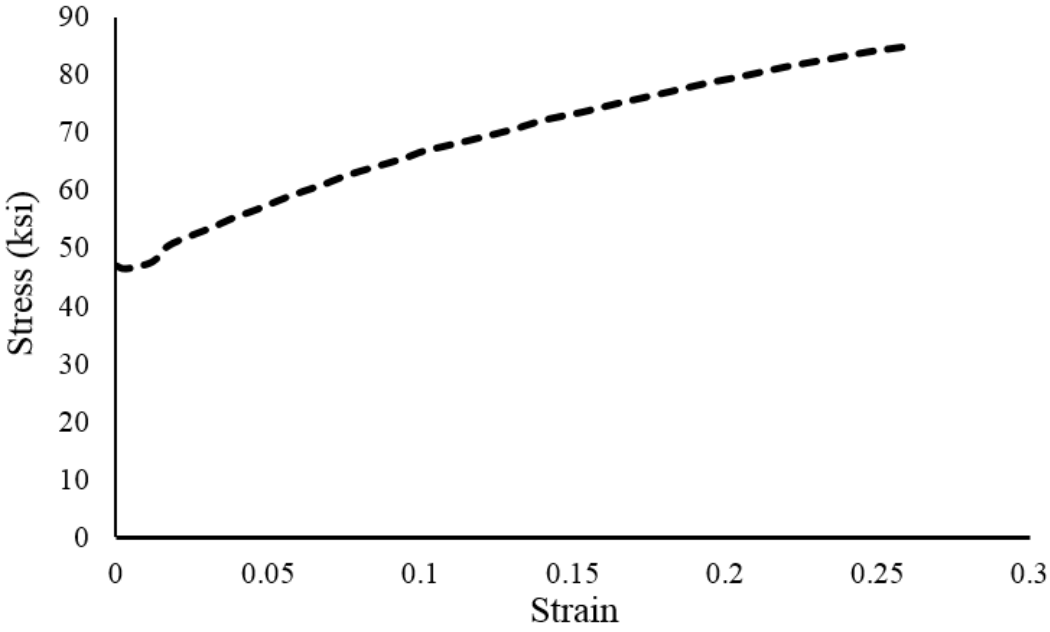

Figure 15. True stress strain curve for ST44 material.

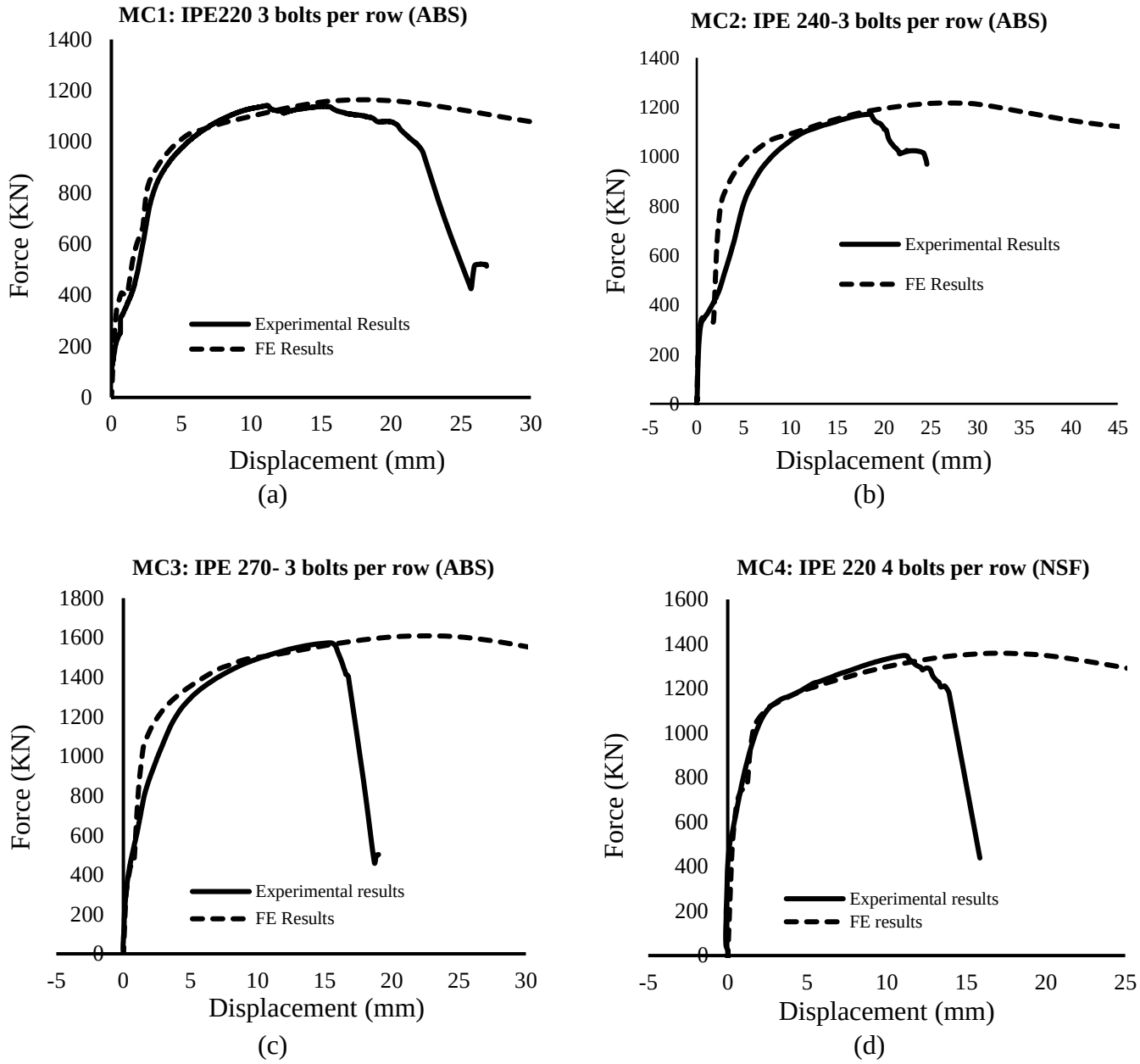

Figure 16. Experimental and FE results of the force displacement of (a) MC1, (b) MC2, (c) MC3, and (d) MC4.

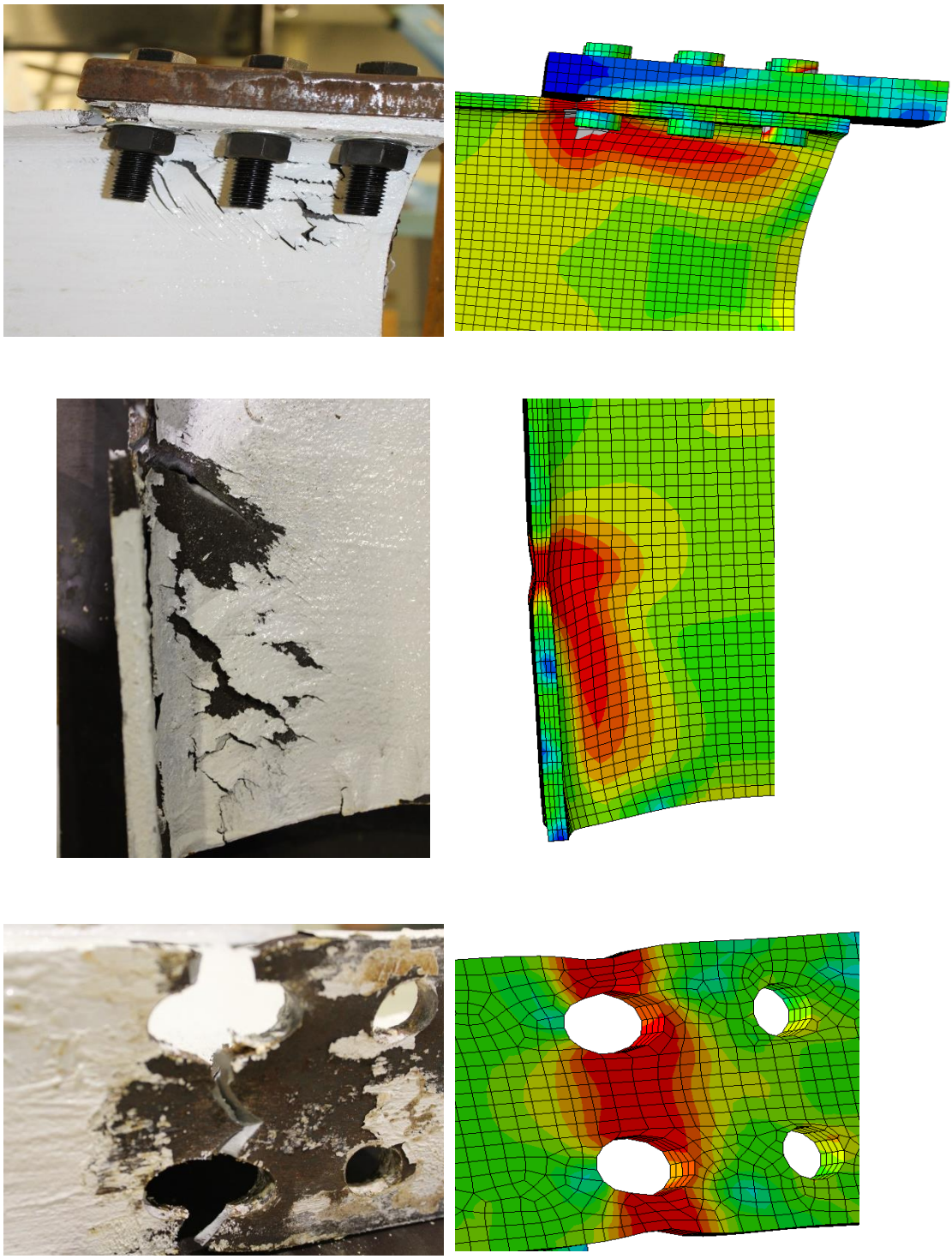

(a)

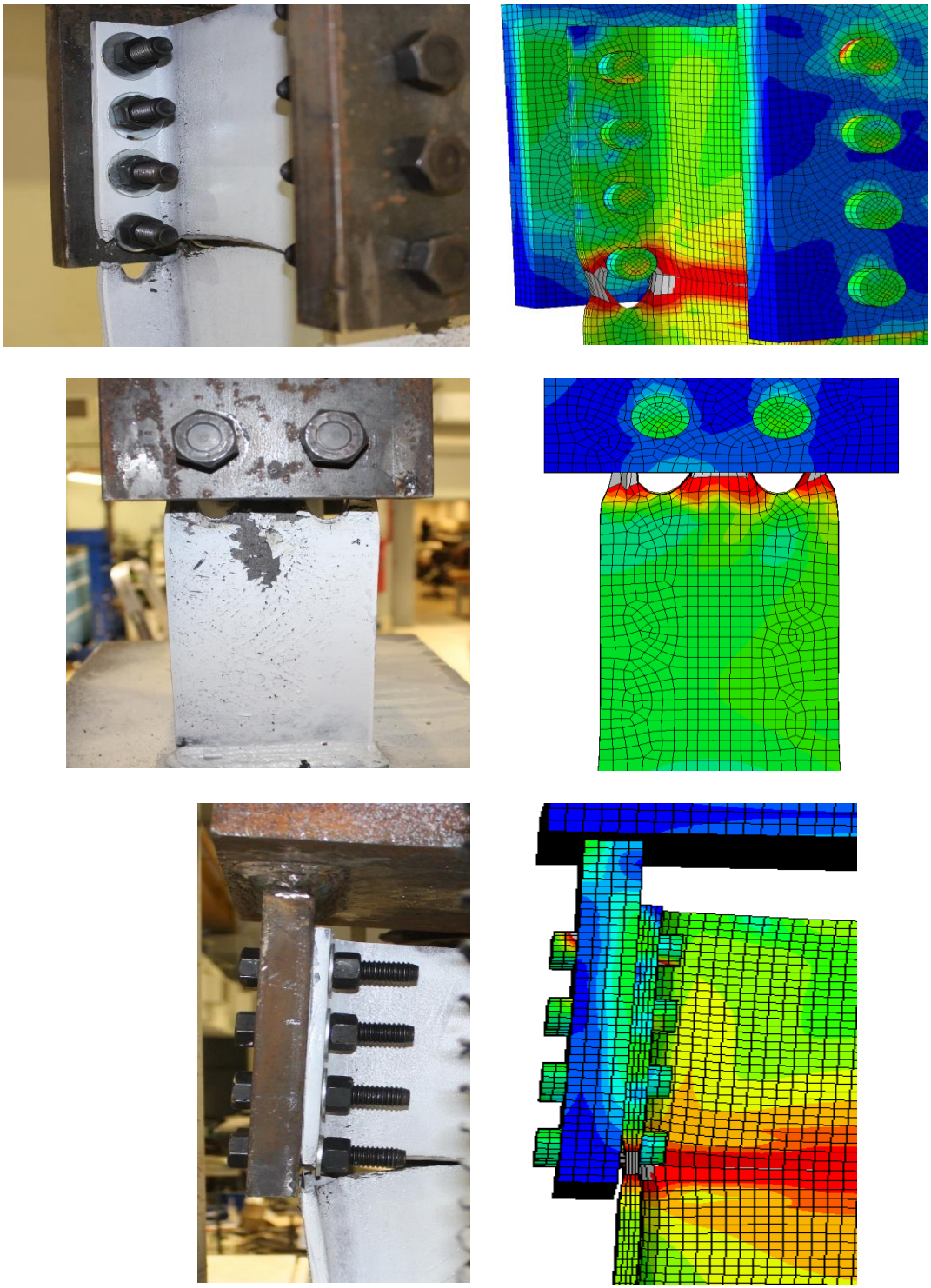

(b)

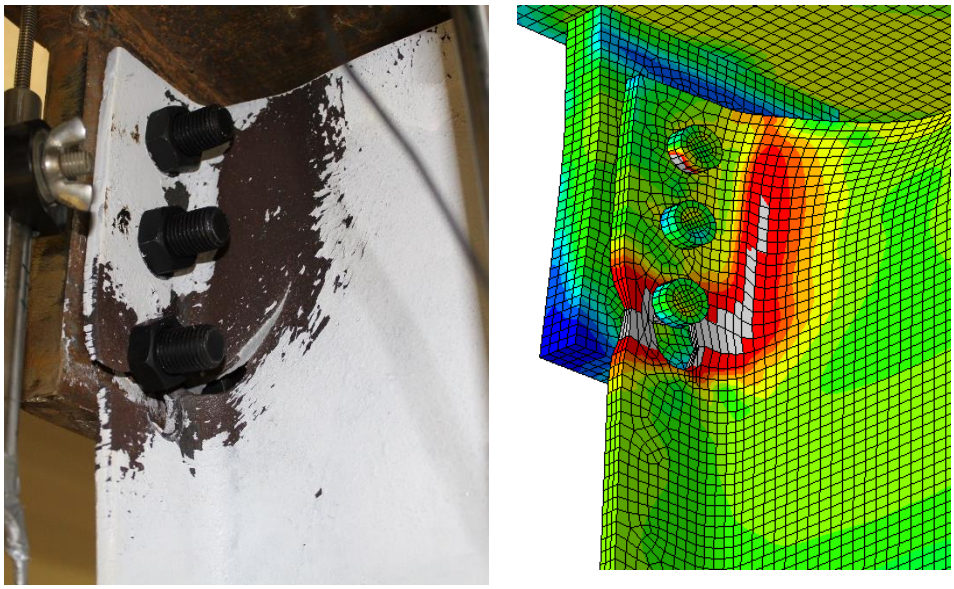

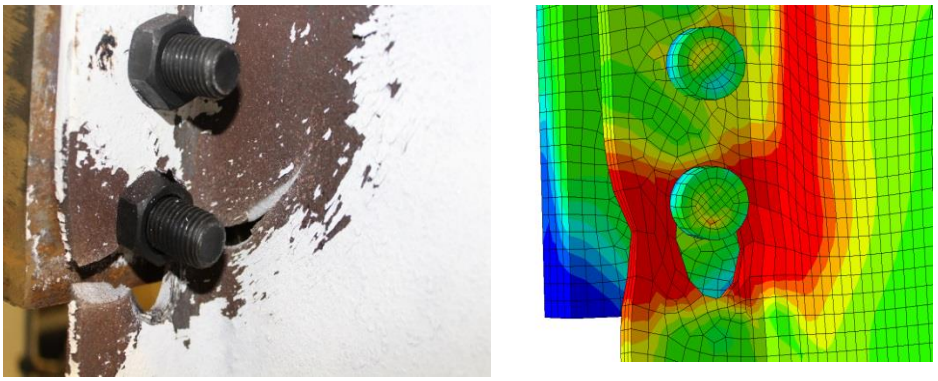

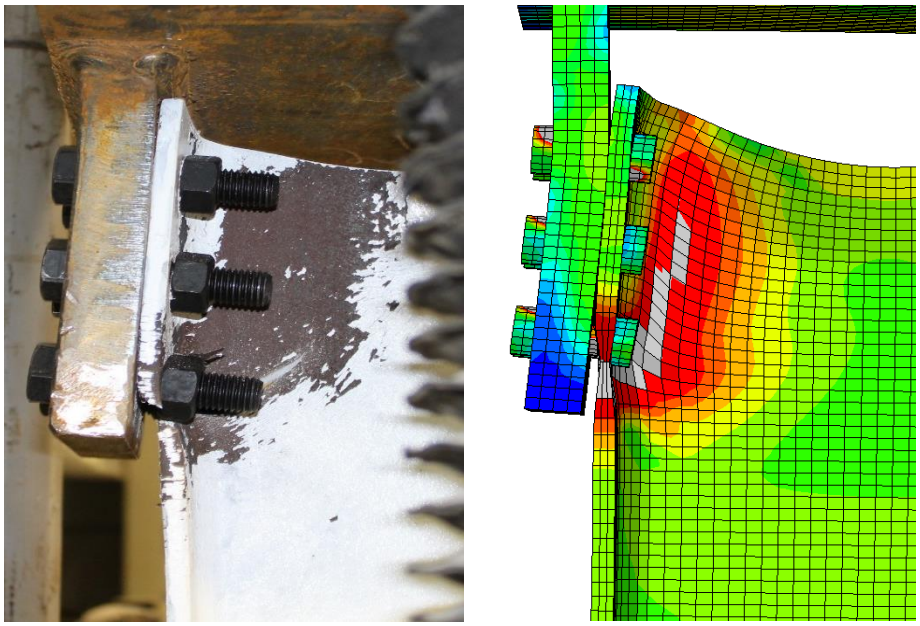

(d)

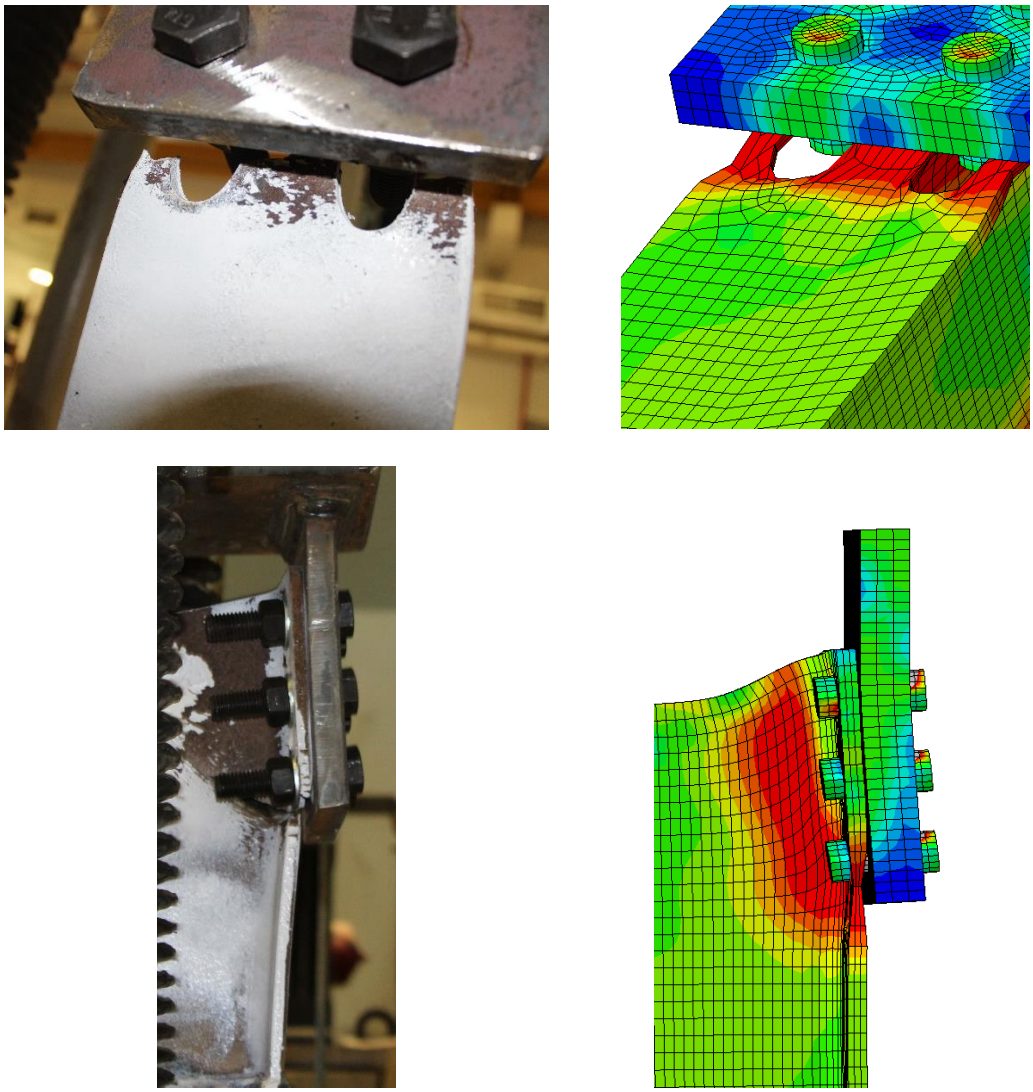

(e)

Figure 17. von Mises contours vs. experimental failure path of (a) MC1, (b) MC2, (c) MC3, (d) MC4, (e).

CHAPTER VII

EXISTING STRENGTH MODELS APPLIED ON STRUCTURAL TEE AND MOMENT CONNECTIONS (BFP AND DOUBLE TEE)

A strength model that predicts the ABS load capacity can be used as design check when designing BFP and double Tee moment connections. The US building code did not yet incorporate strength check for the ABS failure mode. The purpose of this section is to evaluate the capability of existing strength models in prediction of the ABS failure. Existing strength models developed by Epstein (1996), and Driver et al. (2005) and Cai and Driver (2010) are compared with the experimental results of structural Tee connections (Epstein and Stamberg, 2002) and the experimental and FE results of BFP and double Tee moment connections conducted in this study.

The strength model developed by Epstein (1996) is taken as the lesser of the following two equations:

$$R_n = \text{lesser of} \begin{cases} 0.6F_yA_{gv} + F_uA_{nt} & (13a) \\ 0.6F_yA_{nv} + F_uA_{gt} & (13b) \end{cases}$$

where A_{gv} is the beam gross shear area, A_{nv} is the beam net shear area, A_{gt} is the beam gross tension area, A_{nt} is the beam net tension area , F_y is the steel yield stress, and F_u is the steel ultimate stress.

The work performed by Epstein (1996) provided adjustments on the shear area and the tension area of the block shear equation available in the ANSI/AISC 360 specifications (ANSI/AISC 360, 2010). The areas necessary for the calculation of ABS capacity are modified as follow:

$$A_{gv} = A_{nv} = (l + e)t_w \quad (14a)$$

$$A_{gt} = A_g - (d - k)t_w \quad (15b)$$

$$A_{nt} = A_{gt} - 2\left(d_b + \frac{1}{16}\right)t_f \quad (15c)$$

where l is the total length of the spacing between the bolts (connection length), e is the beam edge distance, t_w is the beam web thickness, A_g is the beam gross area, d is the beam depth, k is the fillet distance, d_b is the bolt diameter, and t_f is the beam flange thickness.

Another strength model is developed by Driver et al. (2005) and Cai and Driver (2010) to predict the ABS capacity. This strength model (*unified* equation) is given by:

$$R_n = R_t A_{nt} F_u + R_v A_{gv}\left(\frac{F_y + F_u}{2\sqrt{3}}\right) \quad (16)$$

where R_t and R_v are the mean stress correction factors of tension area and shear area, respectively.

The *unified* strength model take into account that the rupture of the tension plane take place on the net area. The shear stress is taken as the average of the shear yield and ultimate stresses, since the capacity can exceed the shear yielding (Driver et al. 2005).

For the case of BFP and double Tee moment connections, all the equations above remain the same except for Eq. 14(a) and 14(b) that become as follow, respectively:

$$A_{gv} = A_{nv} = 2(l + e)t_w \quad 17(a)$$

$$A_{gt} = A_g - (d - 2k)t_w \quad 17(b)$$

A small modification is applied, the "2" coefficient is added in both equations to represent the two shear planes and the two tensile planes (W beams sections) in Eq. 17(a) and 17(b), respectively. Table 6 shows the results of the strength model proposed by Epstein (1996) and the *unified* strength model (Driver et al. 2005 and Cai and Driver,

2010). The most accurate strength model has to have the mean test-to-predicted (T/P) ratios to be the closest to 1.0, and the smallest coefficient of variation (COV). The test-to-predicted ratio is calculated by dividing the failure load provided from the experimental tests (Epstein and Stamberg, 2002) and the FE results by the one resulted from the mentioned existing strength models. It can be seen that the *unified* strength model has a mean test-to-predicted ratios with the closest value to 1.0, and has the smallest coefficient of variation. This indicates that the *unified* strength model (Driver et al. 2005 and Cai and Driver, 2010) is accurate in predicting the ABS capacity when occurring in the structural Tee connection and the steel moment connections (BFP and double Tee).

The main conclusion that can be drawn from the results presented in Table 6 is that the *unified* strength model provides more accurate results than the one provided by Epstein (1996) in predicting the ABS failure load. Therefore, the *unified* strength model by Driver et al. (2005) can be used to accurately predict the ABS capacity in BFP and double Tee moment connections.

Table 6. Failure load capacity of the tested tees (Epstein and Stamberg, 2002) and moment resisting connections that failed under ABS using *unified* equation (Driver et al. 2005, and Cai and Driver, 2010), and Epstein equation (Epstein, 1996)

	Specimen name	Test results		*Unified* strength model[2]		Epstein strength model[3]	
		Failure mode	Failure load KN (kips)	Capacity load KN (kips)	Test-to-predicted (T/P)	Capacity load KN (kips)	Test-to-Predicted (T/P)
Series[1]	E1	ABS	388 (87.3)	350 (78.7)	1.11	334 (75.2)	1.16
	E1/C1	ABS	379 (85.1)	350 (78.7)	1.08	334 (75.2)	1.13
	E1/C2	ABS	363 (81.7)	350 (78.7)	1.04	334 (75.2)	1.09
	E1/C3	ABS	386 (86.8)	350 (78.7)	1.10	334 (75.2)	1.15
	E2	ABS	431 (97)	383 (86.14)	1.13	437 (98.2)	0.99
	E5/C8	ABS	398 (89.5)	401 (90.22)	0.99	381 (85.7)	1.04
	E5/C8	ABS	415 (93.3)	401 (90.22)	1.03	381 (85.7)	1.09
	E5/C8	ABS	416 (93.6)	401 (90.22)	1.04	381 (85.7)	1.09
	E5	ABS	409 (91.9)	401 (90.22)	1.02	381 (85.7)	1.07
	E5	ABS	408 (91.7)	401 (90.22)	1.02	381 (85.7)	1.07
	E5	ABS	405 (91.1)	401 (90.22)	1.01	381 (85.7)	1.06
	E5	ABS	390 (87.6)	401 (90.22)	0.97	381 (85.7)	1.02
	C8	ABS	490 (110.1)	809 (114.41)	0.96	496 (111.6)	0.99
	E6	ABS	601 (135.1)	450 (101.15)	1.34	417 (93.8)	1.44
FE models	BFP-1	ABS	7993 (1797)	7055 (1856.00)	1.03	7879 (1771.3)	0.98
	TEE-2-B6	ABS	5480 (1232.05)	5566 (1251.46)	1.02	5332 (1198.8)	0.977
	BFP-3-D40	ABS	1288 (2762.67)	12588 (2830.00)	1.02	12068 (2713.1)	0.98
	TEE-1-D35	ABS	8779 (1973.65)	8953 (2012.73)	1.02	8509 (1913)	0.97
	TEE-3-B7	ABS	10864 (2442.48)	10994 (2471.63)	1.01	10510 (2362.8)	0.97
Specimens experiment	MC1	ABS	1141 (257)	1117 (251)	1.021	1058 (238)	1.078
	MC3 (A36)	ABS	1171 (263)	1148 (258)	1.020	1105 (249)	1.059
	MC4	ABS	1574 (354)	1570 (353)	1.002	1423 (320)	1.106
	Mean test-to-predicted (T/P)				**1.044**		**1.069**
	Mean coefficient of variation (COV)				**0.077**		**0.109**

[1]The series of experimental tests correspond to the ones available in (Epstein and Stamberg, 2002).
[2]The *unified* strength model corresponds to the one available in (Driver et al. 2005, and Cai and Driver, 2010).
[3]Epstein strength model corresponds to the one available in (Epstein, 1996).

CHAPTER VII

ALTERNATE BLOCK SHEAR VS. BLOCK SHEAR

As mentioned earlier, the ANSI/AISC 358-16 (ANSI/AISC 358, 2016) requires designers to check for block shear failure in the beam flange for both BFP and double Tee moment connections. However, the code states that ABS failure needs not be checked. For this reason, a comparison was made between the failure loads of ABS and block shear and it was shown that the ABS failure mechanism is more critical than the block shear and thus needs to be codified in the studied moment connections.

The ANSI/AISC 360-16 (ANSI/AISC 360, 2016) specifications provide the following equation to calculate the block shear capacity:

$$R_n = \text{lesser of} \begin{cases} 0.6F_yA_{gv} + U_{bs}F_uA_{nt} & 18(a) \\ 0.6F_uA_{nv} + U_{bs}F_uA_{nt} & 18(b) \end{cases}$$

where U_{bs} is the shear lag factor and its value can be found in the ANSI/AISC 360-16(ANSI/AISC 360, 2016).

Table 7 shows the comparison between the existing strength models that predict the ABS failure [3, 6] and the block shear equations available in ANSI/AISC 360-16(ANSI/AISC 360, 2016). As mentioned in this study, experimental results showed that ABS governed the behavior of MC1, MC2, and MC3 specimens. Also, the existing strength models showed excellent accuracy in predicting the ABS failure load. The results of the comparison clearly show that the ABS failure mode has a lower capacity than the block shear failure mode for both experimental results and strength models predictions.

Additionally, the strength models were applied on a series of design examples available in the literature of BFP moment connections (BFP1, BFP2, and BFP3) (Sato et al. 2008), and double Tee moment connections (TEE1, and TEE2) (Hantouche, 2010) and compared with the block shear equations as shown in Table 7. The five specimens (BFP and double tee connections) were associated with deep beams W30×108 (BFP1), W30×148 (BFP2), W36×150 (BFP3), W30×108 (TEE1), and W24×76 (TEE2). Note that, these moment connections were designed following the guidelines available in ANSI/AICS 358 in its earlier versions. The geometry and material properties of BFP and double Tee moment connections can be found in (Sato et al. 2008) and (Hantouche, 2010), respectively. Results show that the block shear capacity is greater than the ABS capacity for all the cases (Table 7).

In conclusion, ABS failure has one shear plane in the beam web compared to two shear planes in the beam flange for block shear failure. Recalling that the beam flange thickness is greater than the beam web thickness for the tested specimens and design examples, ABS controlled over block shear failure mode. Thus, it is necessary to consider ABS failure as a potential failure mode and should be included in the design procedure for BFP and double Tee moment connections as a design check.

Table 7. Test results vs. existing strength models **(***unified* strength model and Epstein strength model**)** vs. block shear.

	Specimen name	Test results	ABS *Unified* strength model[1]		ABS Epstein strength model[2]		Block Shear equation[3]
		Failure load KN (kips)	Capacity load KN (kips)	Test-to-Predicted (T/P)	Capacity load KN (kips)	Test-to-Predicted (T/P)	Capacity load KN (kips)
Experimental tests	MC1	1141 (257)	1117 (251)	1.021	1058 (238)	1.078	1241 (279)
	MC2	1171 (263)	1148 (258)	1.020	1105 (249)	1.059	1214 (273)
	MC3	1574 (354)	1570 (353)	1.002	1423 (320)	1.106	1673 (376)
	MC4	1347 (303)	1659 (373)		1521 (342)		2152 (484)
Prequalified BFP moment connections[4]	BFP1		8256 (1856)		7879 (1771)		12801 (2878)
	BFP2		14434 (3245)	N/A	13523 (3040)	N/A	27548 (6193)
	BFP3	N/A	13265 (2982)		12464 (2802)		21405 (4812)
Prequalified double Tee moment connections[5]	TEE1		8483 (1907)		8091 (1819)		12771 (2871)
	TEE2		6454 (1451)		6134 (1379)		10774 (2422)

[1]The *unified* strength model corresponds to the one available in (Driver et al. 2005, and Cai and Driver, 2010).
[2]Epstein strength model corresponds to the one available in (Epstein, 1996).
[3]Block shear equation corresponds to the one available in (ANSI/AISC 360, 2016).
[4]BFP Moment connections corresponds to the one available in (Sato et al. 2008).
[5]Double Tee Moment connections corresponds to the one available in (Hantouche, 2010).

CHAPTER VIII

SUMMARY, CONCLUSIONS AND RECOMMENDATIONS

A. Summary and Conclusions

In designing steel moment connections all failure modes are needed to be accounted for including the ABS failure. In fact, large moment demands in high seismic areas are associated with thick flange plate and Tee stem and large shear bolts in BFP and double Tee moment connections. That is, ABS failure might occur in the beam section. For this reason, experimental and analytical investigations were performed to investigate further the ABS failure in the beams associated with moment connections. Experimental results showed that two different failure modes (ABS and NSF) governed the behavior of the connections depending on the beam depth and connection length. Furthermore, results showed that as the beam depth increases and/or the connection length decreases the failure mode is controlled by ABS. A dimensionless ratio (l/d) is able to predict the governed failure mode (ABS, NSF, or combination of ABS and NSF) in the beams (W24 to W36) associated with BFP and double Tee moment connections. FE models were validated against experimental results and showed excellent prediction of the load-displacement curves and failure paths in all four specimens. Moreover, existing strength models were tested against the experimental and FE results conducted as part of this study. As a result, the *unified* strength model showed excellent agreement with the experimental results and was recommended to be used in predicting the ABS capacity load in BFP and double Tee moment connections. To be able to predict the ultimate path in moment connections whether it is ABS or NSF, a stiffness based model is developed. The proposed stiffness model is able to account for the force displacement of BFP and double Tee moment connections. A comparison between ABS and block

shear capacities showed that ABS is more critical and thus it is essential to include it in the design codes of both moment connections. Also, experimental results showed that ABS is a combination of both yielding and rupture and thus can be considered a ductile failure mode. Furthermore, although ABS might not be the governing failure mode in BFP and double Tee moment connections, it can potentially be the next failure mode after beam plastic hinging. This study resulted in the following conclusions:

- The FE results show that the major parameters impacting the ABS failure in structural Tee connections are the beam depth and the connection length.
- The FE parametric results show that the connection length to beam depth ratio (l/d) is the dimensionless ratio that can predict the governed failure modes (ABS, NSF, or a combination of ABS and NSF) in BFP and double Tee moment connections.
- Experimental results showed two different failure modes (ABS and NSF) that governed the behavior of BFP and double Tee moment connections depending on the beam depth and the connection length.
- ABS failure is reported in this study as a ductile failure.
- The proposed stiffness model is able to account for the governed failure mode (ABS or NSF) based on the connection length to beam depth ratio (l/d). One of the main advantages of the proposed stiffness model is that, it is accurate and it needs less computational effort when compared to FE analysis.
- The *unified* strength model (Driver et al. 2005 and Cai and Driver, 2010) is recommended to be used in predicting the ABS load capacity in BFP and double Tee moment connections. This strength model shows excellent agreement when tested against experimental results available in the literature and FE results conducted in this study.

This research provides the engineers design guidelines in predicting the ABS failure in beams associated with BFP and double Tee moment connections. Moreover, this study is a preliminary step towards including the ABS failure in the provisions and specifications as a potential failure mode that needs to be checked. Finally, the performed experimental and analytical investigations are part of an ongoing research that aims at codifying the ABS failure mode in BFP and double Tee moments connections to ensure a safe design.

B. Recommendations

More research work is still needed in order to develop a full understanding of the ABS behavior in moment resisting frames.

- A fracture model to be incorporated in the FE simulations to allow the prediction of the behavior of the connection post-ABS failure.
- Investigation of the ABS in steel moment connections when welding is used instead of shear bolts has to be conducted.
- More experimental tests are needed to be conducted in order to include a full scale moment connections (BFP and double Tee connections) with deep beams ranging between W24 and W36.

BIBLOGHRAPHY

American Institute of Steel Construction (AISC). (2010). "Specification for structural steel buildings." *ANSI/AISC 360-10*, Chicago, IL.

American Institute of Steel Construction (AISC). (2005). "Prequalified connections for special and intermediate steel moment frames for seismic applications." *ANSI/AISC 358-05*, Chicago, IL.

Cai Q., Driver R., (2010). "Prediction of Bolted Connection Capacity for Block Shear Failures along Atypical Paths." *Engineering Journal*, pp. 213-221.

Driver R., Gordin G., Kulak G. (2006). "Unified block shear equation for achieving consistent reliability." *Constructional Steel Research*, pp. 210-222.

Epstein H. (1996). "Block shear of structural tees in tension - alternate paths." *Engineering Journal*, pp. 228-239.

Epstein H., McGinnis M. (2000). "Finite element modeling of block shear in structural tees." *Computers & Structures*, pp. 571-582.

Epstein H., Stamberg H. (2002). "Block Shear and Net Section Capacities of Structural Tees in Tension: Test Results and Code Implications." *Engineering Journal*, pp. 228-239.

European Committee for Standardization (CEN). (2005). "Eurocode 3: Design of Steel Structures --- Part 1-8: Design of Joints and Building Frames." *BS EN 1993-1-8*, Brussels.

Hantouche E., (2011). "Behavior of Thick Flange Built-up T-stub Connections For Moment Resisting Frames." University of Cincinnati, Cincinnati, Ohio.

Hantouche G., Jaffal H. (2016). "Design of Thick Plate Double- Tee Connections for Seismic Applications." *Practice Periodical on Structural Design and Construction*, vol. 21, no. 4.

Sato A., Newel D., Uang C., (2008). "Cyclic Behavior and Seismic Design of Bolted Flange Plate Steel Moment Connections." *Engineering Journal*, pp. 221-232.

Wuwer W., Zamorowski J., Swierczyna S., (2012). "Lap joints stiffness according to Eurocode EC3 and experimental investigations results." *Archives of civil and Mechanical Engineering*, pp. 95-104.